MASTER THESIS

Modelling for Science and Engineering

Changes in Barcelona air quality during the COVID-19 Pandemic using the WRF-Chem model

Universitat Autònoma de Barcelona

Macià Mut Sbert

September 2021

Directors: **Alba Badia Moragas and Gara Villalba Méndez**

Universitat Autònoma de Barcelona - 9 September 2021

Abstract

Lockdown measures during COVID-19 pandemic have supposed a drastic drop of antropoghenic emissions. This exceptional situation provided the opportunity assess a unique large-scale experiment in terms of air quality. The aim of this project is to evaluate the effect of these emission reductions using data given by the WRF-Chem model and compare data observed during the different stages of lockdown (from March 1^{st} of 2020 to April 10^{th} of 2020): pre-covid stage, lockdown stage and full-lockdown stage. To do so, we study five pollutants, PM_{10} and O_3 as principal targets of the study and NO, NO_2 and CO for their role in the chemical production of ozone, computing their time evolution during the whole period and the aggregated daily profile in each stage. We see that the model underestimates the concentrations of the primary pollutants (PM_{10}, NO and NO_2) while overestimating ozone levels (a secondary pollutant), compared to observational data. In the same way, the variations in pollutant concentration are underestimated for all the studied air pollutants. Model results show variations of +1.84% (PM_{10}), +1.81% (O_3), -12.53% (NO_2) and -15.87% (NO). On the other hand, respective observed variations are quite larger: -27% (PM_{10}), +28.8% (O_3) and -47.0% (NO_2) [1] Results for CO show an anomalous behaviour of the concentration of the air pollutant that would require a deeper analysis beyond the scope of this project. So, even though it is not taken into account in our overall analysis, we perform a brief individual discussion on its results.

[1]Results presented in [5]. The study does not present data for NO.

Acknowledgements

First of all, I want to thank the URBAG group for providing us with modelled data we used in this project. Also, I would like to express my great appreciation to Dra Alba Badia Moragas and Dra Verònica Vidal Canedo for all their guide and assistance. Specially, I want to congratulate them on their maternity and thank them the effort on always finding time attending me at all times. Finally, I want to thank my parents and specially Petra for their emotional inconditional support during the progress of these work.

Contents

List of Figures

List of Tables

1 Introduction

On March 2020, the World Health Organization (WHO) declared the COVID-19 pandemic which global-scaled impact consisted on more than 100 million infections and more than 2 million deceases by January the 20^{th} of 2021 [1]. In order to mitigate its effects national governments imposed lockdown measures consisting basically on mobility restrictions. It has been estimated that retail and recreational mobility have drop drastically in Spain, reaching 80% reductions in traffic zones in Barcelona [2].

This exceptional situation allowed the evaluation of the effects of massive road traffic reduction in a large scale experiment. In fact, current results on this matter show that pollutant concentrations have decreased in the in cities around the world where lockdown measures were adopted. An study comparing $PM_{2.5}$ levels before and after the start of lockdown, point to an average reduction of 12% among the 50 most polluted cities in the world [3]. Besides, an air quality improvement has been seen in India during the lockdown period respect to the same dates of previous years. Indian cities recorded decreases in $PM_{2.5}$ (-43%), PM_{10} (-31%), NO_2 (-18%) and CO (-10%). However, a 17% increase in ozone levels was also recorded [4]. Similar behaviors occur in Barcelona, where reductions reaching about -50% for NO_2, -31% for PM_{10} and -45% for black carbon beside a remarkable +57% increase in ozone concentration were computed [5].

So, as a general trend, the lockdown restrictions result in a decrease of primary pollutants like PMs, NO_2 and CO (directly emitted), but also with an increase of ozone, which is not directly emitted but created in the atmosphere by a complex photo-chemical process. This unexpected ozone pollution is discussed in [6]. All in all, the presented results show a positive view to the situation showing an improvement in air quality and helping us in the design of efficient air quality policies.

Bad air quality is a public health problem around the world. According to WHO estimations, long term exposure to highly polluted air is responsible for more than 4.2 million premature deaths as well as for the developing of respiratory and cardiovascular diseases [7]. Moreover, recent studies indicate that poor air quality conditions can worsen COVID-19 effects ([8], [9]) Also, it has been speculated on how pollution can enhance the pandemic spreading hypothesizing the possibility that SARS-CoV-2 RNA could be attached to $PM_{2.5}$ particles [10]. Air quality studies can be complemented with atmosphere dispersion models as it is done in [4] using the Air Quality Dispersion Modelling System (AERMOD) [11]. Such models simulate how pollutants disperse in the atmosphere by implementing its ruling transport equations. The usage of dispersion modeling allow to estimate and predict pollutant concentrations in a region enriching air quality assessment. It exists a vast collection of dispersion models. Most of them can simulate the transport of any pollutant or particle like AERMOD [11] or CHIMERE [12] models. In addition, there are more specific models such as BSC-DREAM8b [13], which is used primary for dust daily forecasting, or the EMEP/MSC-W model concerned with ozone and particulate matter at European regional scale [14]. This models usually couple with the WRF model (*Weather Forecasting Model*) (WRF-AERMOD, WRF-CHIMERE). Doing so, pollution transport simulations can be performed simultaneously with meteorological predictions.

In this project we work with atmospheric data simulated by the WRF-Chem model. WRF-Chem combines the Weather Forecasting Model with its Chemistry (Chem) exten-

sion which enables atmosphere chemical analysis. So, WRF-Chem can be used as an air quality model, despite its usage scope is larger [15].

The URBAG group has designed two runs of the model in the scope of an ongoing project. On one hand we find the *BAU simulation* accounting for a business as usual situation. On the other hand, the *COVID simulation* is designed taking into account the emission reductions recorded during lockdown periods. Then, the objective of this work is to quantify the changes in air quality using simulated data. In addition, this study assesses the performance of the model comparing its predictions with 2020 observational data.

This analysis is performed in the city of Barcelona for the first lockdown weeks (from the 16^{th} March to the 10^{th} April of 2020) and we include also data of the two previous weeks to evaluate the model. It is important to state that we do not aim to present a complete overview on air quality changes, but we focus principally on two pollutants, PM_{10} and O_3, which are two of the most concerning pollutants in Barcelona [16].

This document is organized in six sections. Firstly, we present the Metropolitan Area of Barcelona (AMB) along with an overview of the air quality conditions in the past few years (Section 2). Secondly, the characteristics and health effects of the chosen pollutants are explained. Then, we explain the followed methodology of our work (Section 4). Next, the results are presented distributed in two sections. We present first the evaluation of the model (Section 5) followed by the results of our work with their discussions (Section 6). Finally, we include some conclusions on our study and further steps proposals (Section 7).

2 Air Quality in the *AMB*

The Metropolitan Area of Barcelona, or more commonly *AMB* for its acronym in Catalan (*Àrea Metropolitana de Barcelona*), is the aggregation of towns and cities surrounding Barcelona that in territorial, social, demographic, economic, cultural terms mean a metropolitan unit. The AMB is organized as a public administration constituted by thirty-six town councils that take up over 636 km^2 [17].

The economic activity of the city of Barcelona, based on commerce and tourism, causes an important movement of people and goods within the AMB and out of it. Due to this fact, both the port and airport of Barcelona have a high flow of operations, making them two of the most active stations in the Mediterranean. In addition, the AMB has a road system capable of absorbing the current traffic intensity.

All in all, the traffic volume in the AMB harms air quality, being the most predominant source of primary pollutant emissions. Traffic emissions mean the 85% of PM_{10} emissions and almost the 60% of NO_x emissions [18].

The exposition to bad air quality conditions makes pollution one of the main problems in terms of public health in Barcelona and its whole Metropolitan Area. According to the Air Quality Report of 2019 [19], it is estimated that the high levels of atmospheric pollution are the cause of the 7% of natural deaths, the 11% of new lung cancer cases, and also, the cause of the 33% of new childish asthma. Furthermore, beyond respiratory difficulties, other adverse effects caused by poor air quality include cardiovascular diseases and detrimental issues in baby development during pregnancy.

2.1 Air Quality measuring

In the last years, the World Health Organization (WHO) has developed a quantitative system to evaluate air quality and assess the impact of pollution on health [20]. In 2005, the WHO presented the guideline concentration levels of the principal air pollutants. These concentrations define a maximum threshold for chronic exposure to a pollutant [21].

Most pollutants have a short-term threshold, like a daily or hourly maximum, and a long-term one. The second, which is lower, indicate the risk level for persistent exposures in time. The WHO guidelines for the principal pollutants are listed below.

- Coarse particulate matter [2] (PM_{10}):

  Annual mean: $20\,\mu g/m^3$.

  24 - h mean: $50\,\mu g/m^3$.

- Fine particulate matter ($PM_{2.5}$):

  Annual mean: $10\,\mu g/m^3$.

  24 - h mean: $25\,\mu g/m^3$.

- Ozone (O_3):

  8h - mean: $100\,\mu g/m^3$.

- Nitrogen dioxide (NO_2):

  Annual mean: $40\,\mu g/m^3$.

  1h - mean: $200\,\mu g/m^3$.

- Carbon monoxide (CO):

  8h - mean maximum: $10\,mg/m^3$.

  1h - maximum: $30\,\mu g/m^3$.

- Sulfur dioxide (SO_2):

  24h - mean: $20\,\mu g/m^3$.

  10 minute - mean: $500\,\mu g/m^3$.

In Catalonia, Air Pollution Monitoring and Forecasting Network or *XVPCA* for its acronym in Catalan (*Xarxa de Vigilància i Predicció de Contaminació Atmosfèrica*), is the network associated with the Catalan Government responsible for measuring the pollution concentrations all over the territory. To do so, it has a deployment of measuring stations strategically positioned in the most troubling points in terms of air quality. Among these, stands out the city of Barcelona and, to a greater extension, the whole AMB.

The Public Health Agency of Barcelona, or *ASPB* for its acronym in Catalan (*Agència de Salut Pública de Barcelona*), which is the institution responsible for the evaluation

[2] A more detailed explanation on particulate matter and its types is presented in Section 3.

of air quality in Barcelona among other issues, present yearly reports on this matter. Recent reports ([16], [19]) show how the WHO guideline levels exceeded in most traffic stations for NO_2, PM_{10}, $PM_{2.5}$ and O_3. We present a more detailed definition of the type of stations in Section 4. Briefly, a traffic station is a pollution measurement station set in a spot where traffic is the principal emission source.

Table 1 shows the number of times the WHO thresholds exceeded in Barcelona, according to the previously mentioned reports. In the mentioned tables, *Exceeded* means that the WHO guideline value has been exceeded at least at one of the stations. *Not exceeded*, on the other hand, is used when the threshold value has not exceeded in any station ([16], [19]).

	Traffic stations	Background stations
NO_2 year average	Exceeded (2)	Not exceeded
PM_{10} year average	Exceeded (3)	Exceeded (5)
$PM_{2.5}$ year averge	Exceeded (3)	Exceeded (4)
O_3 8 - hour maximum	Exceeded (2)	Exceeded (3)
CO 8 - hour maximum	Not exceeded	Not exceeded
CO hourly maximum	Not exceeded	Not exceeded
SO_2 daily maximum	Not exceeded	Not exceeded

Table 1: WHO thresholds that were exceeded in 2018 and 2019 (ASPB). In parenthesis the number of stations that registered pollution overcoming. Data extracted from [16] and [19].

As seen in Table 1 for particulate matter and ozone, the WHO thresholds exceeded in both traffic and background stations in 2018 and 2019. Also, the annual average concentration of NO_2 exceeded in both years. These results show that in business as usual condition Barcelona has a severe problem with pollution.

2.2 Air Quality during COVID-19 period

The outbreak of COVID-19 at the start of the year 2020 had a significant impact on the atmosphere situation and specifically on air quality [5]. The lockdown measures imposed by national governments that implied severe mobility restrictions resulted in a remarkable reduction of emissions. And, to a greater extend, an improvement in air quality. The city of Barcelona was no exception. In fact, he measures adopted by the Spanish National Government are found among the most strict in Europe ([22], [23]).

Data from the XPVCA in the ASPB yearly report point to a concentration decrease for all principal pollutants attributable to lockdown restrictions. When comparing to pre-COVID period levels, during the strictest lockdown period there are reductions of 43% for NO_2, 21% for PM_{10}, and 24% for $PM_{2.5}$ [24]. Moreover, according to assessments of the ASPB, the exposure of the population to NO_2 and $PM_{2.5}$ has reduced by 28% and 23%, respectively.

As a result of these emission reductions, the concentration of NO_2 has remained under the threshold set by the WHO. [21] However, despite the air quality improvement, the WHO guideline levels were still exceeded for PM_{10} in 3 traffic and 5 background stations, for

$PM_{2.5}$ in 3 traffic and 4 background stations and for ozone in 2 and 3 stations, traffic and background respectively. it has not been achieved to reduce the PMs and O_3 pollution levels to WHO guideline levels. For both pollutants, these thresholds exceeded in Even though, these excesses were lighter than in past years ([16], [19], [24]).

3 Air pollutants and their sources

In this project we focus our work in the analysis of coarse particulate matter (PM_{10}) and ozone (O_3). This choice is based on two main reasons. On the one hand, the effect of COVID lockdown on the concentration levels of these two pollutants has not been already deeply discussed in the city of Barcelona, where there is an actual pollution problem related to them. At least, at the time this project was proposed. This is not the case of NO_2, for which we can find such analysis in the literature, [25].
On the other hand, in order to get a more complete assessment of the performance of the model designed by URBAG, we study a primary pollutant as it is PM_{10} and a secondary pollutant like O_3.
The term primary pollutant is referred to a pollutant that is directly emitted by some source like road traffic. A secondary pollutant on the contrary is a pollutant agent that is formed in the atmosphere as a result of a chemical procedure, usually triggered and derived from an excess of primary pollutants.

3.1 Coarse Particulate Matter, PM_{10}

The general term particulate matter (PM) refers to an ensemble of aerosols of different composition, distribution, size, toxicity and origin. These particles can be found in solid, liquid or solid and liquid state [26]. The classification of particulate matter is based on the aerodynamic properties of the particles. Such properties are collected in the aerodynamic diameter that is defined as the diameter of a unit-density sphere with the same aerodynamic properties [21].

Nowadays, the WHO distinguishes between two PM pollutant agents depending on their aerodynamic size. The fine particulate matter or $PM_{2.5}$, particles with a diameter $< 2.5\,\mu m$. And coarse particulate matter or PM_{10} that includes particles with an aerodynamic diameter between $2.5\,\mu m$ and $10\,\mu m$ [21]. We do not include $PM_2.5$ in our study because it is only monitored by two XVPCA stations in the whole Catalan territory, preventing us from having a rich statistical analysis of its behaviour [27]

The composition of these particles is heterogeneous and depends on the studied geographic area nature and the antropogenic emission sources in the region ([28], [29], [30]). In the city of Barcelona, the PM_{10} is caused virtually even by traffic emission, industrial emissions and crustal dust [26]. This last pollution source includes dust coming from erosion and particles lifted in suspension by road traffic. Therefore, it can be said that such dust is an indirect effect of traffic.

3.2 Ozone, O_3

Ozone is a gas known for constituting a layer around the planet that protects the surface from harmful solar radiation. However, its excessive concentration in the troposphere, the lowest layer in the atmosphere, has also harmful effects on human health, the environment and it affects climate change. The same absorbent property that makes it essential for life on Earth, turns O_3 in a greenhouse gas when it is present in the troposphere. Moreover, its oxidant nature has a severe impact on the environment harming vegetation and affecting stages of the water cycle like the evaporation rates and cloud formation [31].

Beside these environmental impacts, high ozone concentrations constitute an urban smog which is detrimental for human health. Long term exposures to such O_3 levels can originate respiratory problems like asthma and lung diseases [32].

Studies from the EEA (European Environment Agency) conclude that the Mediterranean basin is the most affected region by ozone in Europe. The combination of anticyclonic and warm weather conditions, the high pollutant emissions in the region and the dynamics of air masses caused by orographic feature favor the accumulation, stagnation and creation of ozone [33]

Ozone chemistry

As we said, tropospheric ozone is a secondary pollutant, meaning that it is not directly emitted by natural or antropoghenic sources. In our case, ozone is the product of a photo-chemical reaction that occurs in the atmosphere that includes, among others, primary pollutants like NO, NO_2, CO or VOCs, that stands for *Volatile Organic Compounds*, short-lived radicals as RO_2, OH or HO_2 and compounds derived from carbon [34]. An schematic representation of the chemical reactions involved in the formation of ozone is shown in Figure 1. In general terms we can say that the oxidation of CO and more

$$\begin{aligned}
&VOC + OH + O_2 && \circledR && RO_2 + H_2O \\
&RO_2 + NO + O_2 && \circledR && NO_2 + HO_2 + CARB \\
&HO_2 + NO && \circledR && NO_2 + OH \\
&2(NO_2 + h\nu + O_2 && \ll && NO + O_3) \\
&(NOx + OH +)\, VOC + 4O_2 && \circledR && 2O_3 + CARB + H_2O\ (+ NOx + OH)
\end{aligned}$$

Figure 1: Simplified photo-chemistry of ozone (Figure from EEA 1998 report [35]). RO_2, OH and HO_2 represent radicals, *VOC* stands for volatile organic componds and *CARB* for compounds derived from carbon.

significantly the oxidation of VOC are the precursor reactions of ozone formation. So, greater concentrations of these pollutants shall induce a greater production of ozone. These reactions that follows the VOC and CO oxidation are catalyzed by NO and NO_2, that when analyzing this photo-chemical process are usually taken together as NO_x (NO_x = NO + NO_2). In fact, the production rate of ozone depends strongly on the ratio between VOC and NO_x concentrations: the VOC/NO_x ratio.

In urban areas, the high antropoghenic emissions result in high NO_x concentrations and therefore in a low VOC/NO_x ratio. In this regime the concentration of O_3 is conditioned mainly by NO_x tritation. In this photo-chemical process NO reacts with O_3 to create NO_2 and oxygen. So, high concentrations of NO_x induce a decrease on ozone production, and vice-versa [35]. An example of this behaviour is the weekly pattern in ozone levels that has been observed in some Belgian cities. Ozone concentration peaks have been recorded during weekends, when NO_x emissions and concentrations are lower. This phenomenon has been named as the "week-end effect" [36].

All in all, this whole complex chemical process makes the analysis of primary pollutants like NO_2, NO and CO necessary to perfom a proper evaluation of ozone levels and concentrations.

4 Methodology

For our study we combine observational data, provided by the *Xarxa de Vigilància i Predicció de Contaminació Atmosfèrica* (XVPCA), with simulated atmospheric data given by an air quality model. We emphasize that we have not designed or executed these simulations. Their results have been provided by the URBAG group[3]. However, an explanation about the model is necessary for a proper understanding of the project.

4.1 The model

4.1.1 Model description: WRF-Chem

The simulations we are using have been computed with the wide know forecasting community model, the WRF model. It stands for Weather Research and Forecasting model and it is used for both research and operational forecasting. Its vast usage among the scientific community is due to its many applications such as atmospheric physics research, real time numerical weather prediction (NWP) and forecast system research. Besides, it can be coupled with chemistry analysis software (WRF-Chem) [15], as it is done for our simulations, or work with idealized applications at many scales (from hundreds of kilometers to ten meters).
The whole procedure can be split in three parts.

- WRF preprocessing sistem, WPS. It is composed of a set of programs working collectively to prepare the input of the model. That is, WPS handles the interpolation of meteorological data in the WRF grid.
- The WRF model itself which simulates the atmosphere evolution from a set of initial and boundary conditions.
- A set of graphical and verification tools used in furhter analysis.

The WRF model has two dynamical cores: Advanced Research WRF, ARW-WRF, and Nonhydrostatic Mesoscale Model, NMM. Whereas the first can be used in both research

[3]These results are part of an ongoing project.

and NWP while offering idealized cases and other specific tools such as WRF-Chem, NMM is more limited since it is more focused on NWP applications.
These two cores represent the implementation of the model itself and thus include the basic dynamical equations: advection, pressure gradient, Coriolis, buoyancy and diffusion; and also numerical methods for solving these equations like finite differencing or a three-order Runge-Kutta method.

For the simulations we used the ARW dynamical core and particularly, the model coupled online with its chemistry extension WRF-Chem. With WRF-Chem we are able to simulate emission, transport, mixing and chemical transformation of trace gases and aerosols simultaneously with the meteorology [15]. The main benefit of this model is its flexibility when defining the conditions of the simulation. While setting the input of the model we can define the time period of the simulation, the domain and its resolution, the physical characteristics of the model and, of course, the chemistry. Specifically, we can define the different chemical phenomenons and also which chemical species are considered in the simulation and how they react.
Finally, the model output gives a prediction of the atmospheric conditions in our study region and at a given time. Among them we find temperature, pressure, humidity, raining probability and also the synoptic conditions. Moreover, when using the coupled Chemistry extension, the output model gives the predicted values of concentration of the studied chemical species.

4.1.2 Model set-up

The model covers two geographical domains: the Iberian Peninsula using a 9km×9km grid (D1), and the region of Catalonia with a finer grid, 3km×3km (D2), and accounts for 45 vertical layers. In this project, since we restrict our study to the AMB, the results we use correspond to the second domain.

Referring to simulation times, they encompass the period between March 2020 and June 2020. This includes the full length of the lockdown restrictions, from 14th March to the 2nd of May. And also includes the de-escalation process that started on the 2nd of May and extended until the ends of June.

For meteorological data the ERA5 model [37] has been consulted to define the initial atmospheric conditions of the simulations. This database collects data from atmospheric, oceanic and terrestrial variables hourly and has information between 1950 and 2016. The latest release, 2016 data, has been used to set the initial and boundary atmospheric conditions. The ERA5 model data is combined with geographical conditions of the study region as input of the WPS model. Then this pre-processing system interpolates all this data and provides a file with the information in a grid readable to the WRF model.
Similarly, data for the boundary conditions setting has been extracted from the Whole Atmospheric Chemistry Community Model (WACCM) [38]. The WACCM collects information about several chemical species in the atmosphere. For the one hand it provides an open data-set of concentration of such components, mostly pollutants. On the other hand it makes predictions of the behaviour of these chemical species in the atmosphere. WACCM data has been used to set the chemical initial conditions of the simulations. Furthermore, for a complete description of the chemical-atmospheric conditions, information about pollutant emissions is needed. This data has been obtained from the CAMS-

REG-APv3.1 [39] data-set. This is an emission database at European level that provides information about emissions classifying by country and by pollution source. Specifically, the database used corresponds to air pollutant (AP) emissions due to anthropogenic activity at regional scale (REG). The studied pollutants are NO_x, SO_2, NMVOC, NH_3, CO, PM_{10}, $PM_{2.5}$ and CH_4. Version 3.1, the latest release in 2019, correspond to year 2016 emissions.

This data has been pre-processed with HERMESv3 system [40]. This pre-processing model creates emission files readable for atmospheric models, such as WRF-Chem, from emission inventories. HERMES is capable to differentiate between different emission sources and pollutants as well as between geographic regions applying different country-specific mechanisms. The whole set up of the model is summarized in Table 2.

Horizontal resolution	D1: 9km × 9km, D2: 3km × 3km
Period	March - June 2020
Vertical layers	45, up to 100hPa
Chemical initial condition	WACCM [38]
Meteorological initial condition	ERA5 [37]
Emission inventories	CAMS-REG-APv3.1 [39]

Table 2: Experiment configuration

4.1.3 Model runs: COVID and BAU simulations

The model has been run on the cluster *Picasso*. We can access the output data connecting to this cluster where it is kept.
The executions of the model result in two sets of simulations. On the one hand there is the BAU-simulation set. BAU stands for *business as usual* and for this model run a typical rate of emission has been assumed. On the other hand, the COVID-simulation set uses reduced emissions due to mobility restrictions during COVID lockdown. So, in short, the only difference between the two sets are the anthropogenic emissions considered. For the BAU-simulation set, data from the CAMS-REG-APv3.1 [39] data set pre-processed with HERMESv3 is used as it is explained in 4.1.2 [40]. To define the reduced emissions for the COVID-simulation set we use this same data-set but we apply an additional pre-processing step: the reduction factors provided by the Barcelona Supercomputing Center [41] have been applied. In this BSC work Guevara et al. analyzed the emissions during the COVID-lockdown period and, using a machine learning model, estimated the emissions that would occurred if mobility and production restrictions were never imposed. Doing so in different European countries, they have been able to define emission reduction factors for each country, day and pollutant sector.

In Figure 2 we show how the reduction factors for five pollutant sectors evolve during our study period (presented in later section 4.3) in Spain. The sectors here highlighted are: Public Power, Industry, Road Transport and Aviation.
Guevara et al. [41] consider Public Power emissions to be related to energy production, so in some versions of their work this sector is referred as *Energy Industry*. As main assumption, they say that the tendency of these emissions is related to electricity demand. In addition, they define as the most influential factors in such demand the temperature

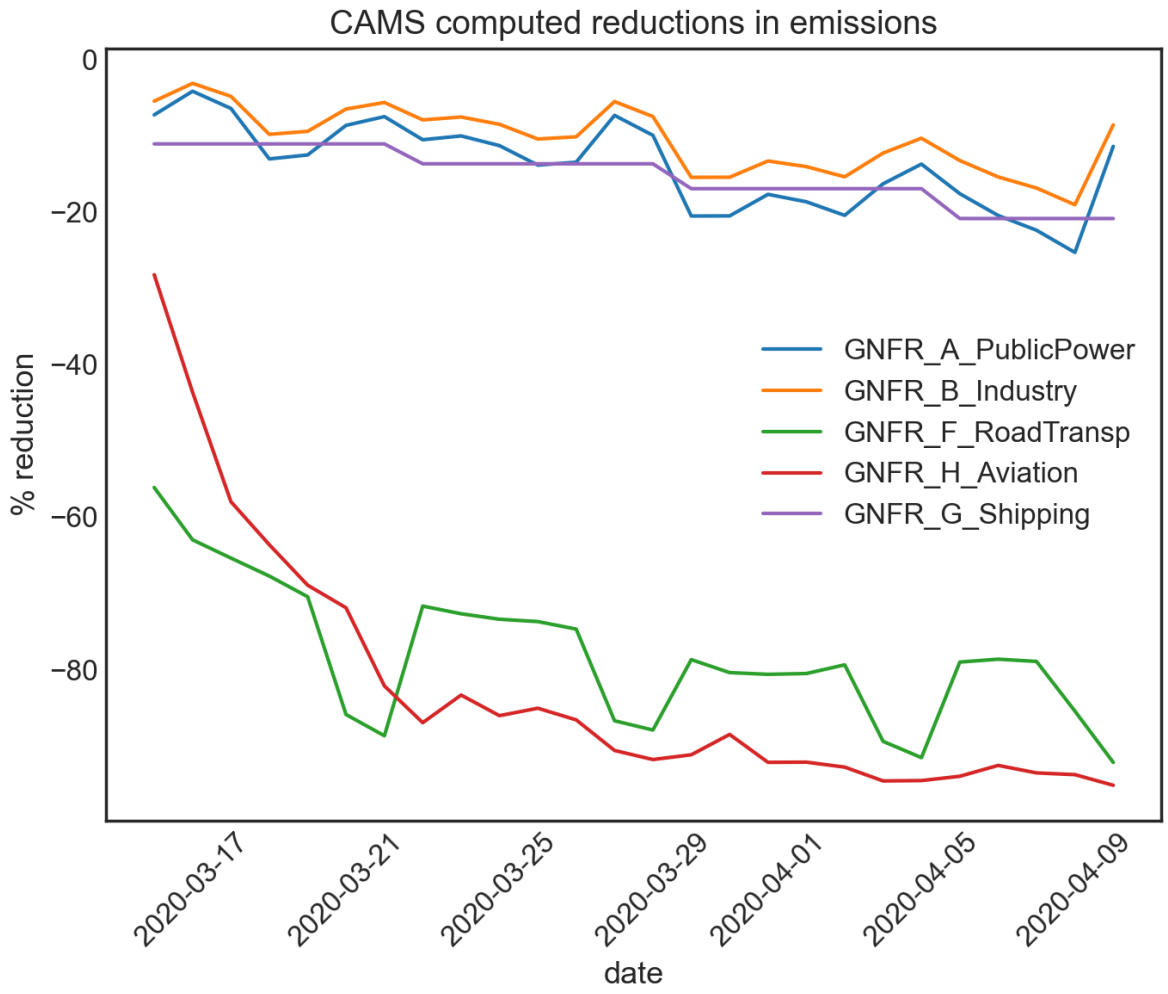

Figure 2: Reduction factors [41] evolution during our study period: from 16$^{\text{th}}$ March to 10$^{\text{th}}$ April. They describe how the emissions of a certain pollutant sector has decreased due to lockdown restrictions, so a negative factor stands for an actual reduction in emissions. Five pollutant sectors have been chosen: Public Power, Industry, Road Transport, Aviation and Shipping.

(heating and air conditioning) and day-week, distinguishing between working or non-working day. In general terms, emission reductions appear when restrictions are imposed. In Figure 2 it can be appreciated a decreasing tendency in the evolution of the reduction factors of this sector, specially there is a sudden decrease when full lockdown [4] is imposed. Moreover, we can identify weekly patterns showing additional reductions during weekends and emission peaks in working days.

For the Industry or *Manufacturing Industry* sector emissions, the same pollutant sources as in the previous sector are considered: energy power plants mainly. In Guevara's et al. it is assumed that a 25% of the total electricity demand reduction to the reduction in manufacturing industry activity. For this reason the behaviour of the reduction factors for this sector follow a similar evolution as the Public Power reduction factors. This can

[4] A more detailed explanation of lockdown and full lockdown situations is presented in later sections

be seen in Figure 2. However, in this figure we can also see that the reductions are smaller for this sector because, even in strict lockdown situations, the industry of essential sectors (food, pharmaceutics) is still active.
From the analysis of these two sectors, Guevara et al. conclude that the reduction in their activity is the main responsible for the decrease in SO_x concentration, [41].

To define the emission reductions due to mobility restrictions in Road Transport in Catalonia (Spain), Guevara et al. [41] analyze mobility date from Google, the *Agència de Tranports Metropolitans* (ATM) and *Dirección General de Tráfico* (DGT). The goal is to identify trends that can give insight of the mobility variation during the lockdown period. It is estimated that road transport mobility has been reduced in a 70%.
As a general conclusion, Guevara et al. say that the emission reductions in this sector are highly correlated with the severity of the imposed restrictions and that they are the main responsible for the reduction of most pollutant concentrations. [41]
In Figure 2 we see a significant reduction as lockdown measures become effective, as it would be expected, and they continue to decrease as more restrictions are imposed. Again, we can identify weekly patterns with slightly higher factors in workdays. This increase is due to essential mobility: heavy-duty transport and displacement to essential work places.
This differences between workdays and weekends reinforce the idea to treat them separately. In fact, in our study period we shall only consider workdays (from Monday to Friday).

For the Aviation sector, only emissions that have direct influence on air quality are considered [41]. That is, only take-off and landing cycles are taken into account. Furthermore, since the contribution of this sector to the total amount of emissions is of the order of 1%, the reduction factors are computed only for the largest airport of each country. The results of this analysis show that the emissions of this sector have reduced in a 90% in all European countries. Such numbers could be expected since movement between different regions and countries was strictly restricted. Indeed, in Figure 2 it can be seen that the greatest decrease is in this sector.

The emissions due to Shipping show a weekly step-wise decrease (Figure 2). This may be because shipping companies keep they week schedules. Moreover, the reductions in this sectors are less pronounced than for Aviation due to the need of constant traffic of essential goods.

In addition, the *Other Stationary Combustion* sector include emissions coming from combustion in residential and commercial energy consumption, for instance fuel combustion in household heating. Differently to the five aforementioned sectors, in this case they provide results for the reduction factors that are pollutant specific. In Figure 3 the evolution of the reduction factors in this sector for each analyzed pollutant in CAMS data-set is shown. As done before, this data concern only to Spanish territory, [41].
In Figure 3 we can distinguish between two behaviours. On the one hand, the pollutants related to wood consumption processed show an slight increase ($\sim 8\%$). In this group we can include NMVOC, CO, $PM_{2.5}$, PM_{10} and NH_3. On the other hand, the other pollutants groups (NO_x and SO_x) experience a moderate decrease.
Again, as it has been seen analyzing the evolution of the reduction factors for the industrial sectors and road transport, a weekly pattern can be appreciated. This pattern shows an slight increase during the week followed by a marked decrease in weekends.

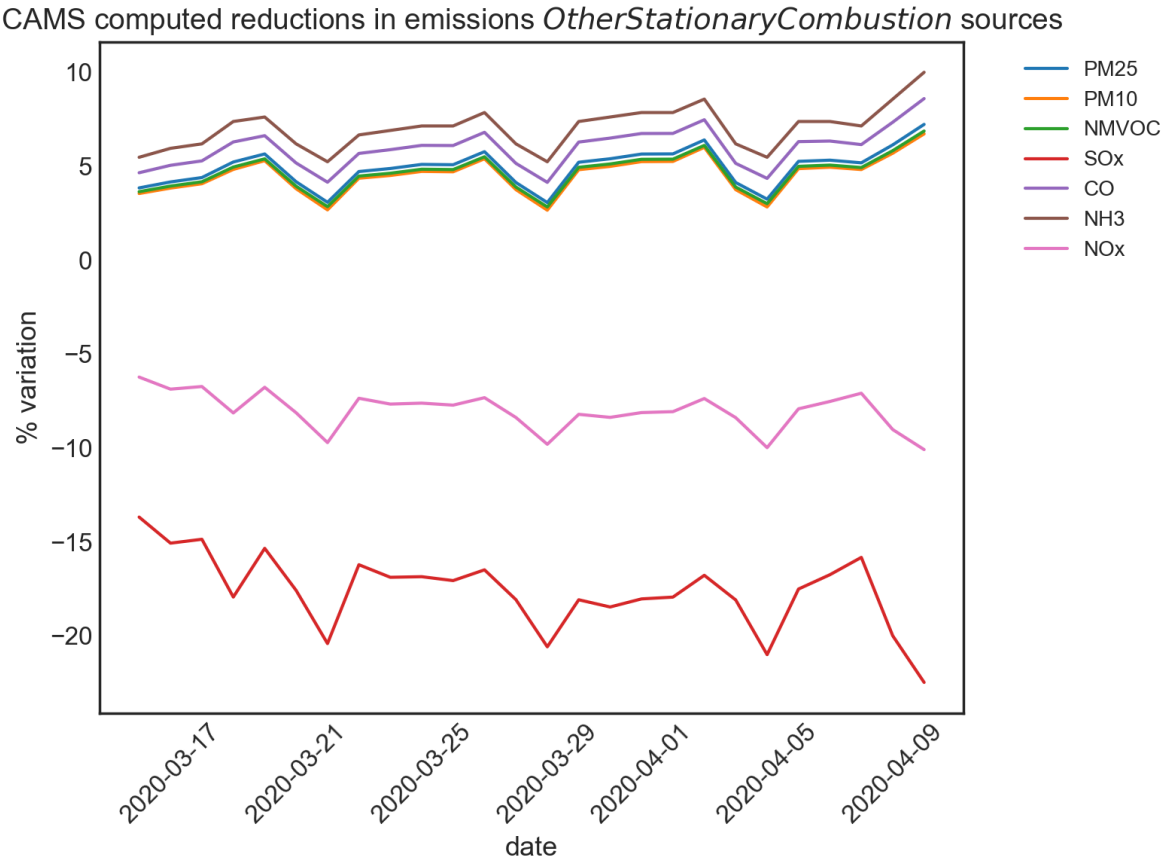

Figure 3: Reduction factors [41] evolution during our study period: from 16$^{\text{th}}$ March to 10$^{\text{th}}$ April. They describe how the emissions for *Other Stationary Combustion* sources have decreased for each pollutant due to lockdown restrictions. So, a negative factor stands for an actual reduction in emissions. Five pollutant sectors have been chosen.

To sum up, we use CAMS-REG-APv3.1 [39] data for the BAU simulations and we apply to this data the emission reduction factor defined by Guevara et al. [41] for the corresponding day, in Catalonia and accounting for all possible polluting sectors.

4.2 XVPCA data. Observations.

We complete our study analysing data from real observations of pollutant concentrations in the atmosphere. As we have already said, this data is provided by the XVPCA. It monitors the principal pollutants (NO, NO_2, NO_x PM_{10}, $PM_{2.5}$, PM_1, O_3, CO, SO_2, H_2S, C_6H_6) and collects insight on their concentration levels. The XVPCA provides open data about all their measurement [27].

A large scale study taking into account data from all the stations would be quite challenging and it is not the aim of this project. Moreover, since road transport (traffic) is the most significant pollutant source in Catalonia and also it is one of the sectors most affected by the lockdown restrictions, we have reduced the scope of our work to the study of air quality in the AMB, presented in Section 2

Within this region we define and particularly analyze four station classes or sectors. To do

so, we combine the two station classifications proposed by the XVPCA. On the one hand, the XVPCA classifies its stations according to the main source of the pollution affecting it. The three types of stations are then: traffic, stations located next to a circulated road; industrial, stations located by an active factory; and finally background stations, which are the ones that measure the remaining pollution in an area. On the other hand, the agency classifies the stations according to its urban area. In this sense, they distinguish between urban, suburban and rural regions.
From the combination of these sectoral and geographical classification, we define the following merged categories:

- Urban - traffic stations.
- Suburban - traffic stations.
- Urban - background stations.
- Suburban - background stations.

We do not include in our study scope neither rural stations, since it is restricted to the metropolitan area of Barcelona (AMB), or industrial stations. This second excluding choice is really subjective because we want to focus on the impact the mobility restrictions had on air quality and on how traffic affects air quality in Barcelona.

	AMB	Urban-Traffic	Suburban-Traffic	Urban-Background	Suburbans-Background
PM_{10}	10	2	1	4	2
O_3	13	2	1	5	5
NO	20	2	2	9	6
NO_2	20	2	2	9	6
CO	8	2	1	2	3

Table 3: Number of stations for each pollutant and defined class, [27].

In Table 3 we present the number of stations there are for each of our defiend classes and for each pollutant. As it is noticed, not all stations gather data for all pollutants. The most monitored pollutants are NO and NO_2, since they are the most abundant and troubling ones ([16], [19]). Whereas, for CO, PM_{10} and O_3 we have significantly less data. Despite this, we consider the total amount of data we can gather from all the AMB to be significant to carry on our study.
Remind that our work is focused on the variations on PM_{10} and O_3 during the COVID-19 pandemic. NO_2 has already been discussed [25] and CO is not as troubling as other pollutants in Barcelona ([16], [19], [24]). However, these gases are necessary to a explain properly the chemistry behind the creation and tritation of ozone in the lower atmosphere, and therefore key for a proper discussion of ozone concentration behaviour [32].

4.3 Studied period

From the whole simulated time, March - June 2020, we restrict our study to the first 41 days of such period, from the 1st March to the 10th April of 2020. For every week in this period, we shall analyze deeper its five working days, see Table 4.

Week	Description
2^{nd} - 6^{th} of March	Pre - lockdown
9^{th} - 13^{th} March	Pre - lockdown
16^{th} - 20^{th} March	Lockdown
23^{rd} - 27^{th} March	Lockdown
30^{th} March - 3^{rd} April	Full lockdown
6^{th} - 10^{th} April	Full lockdown

Table 4: Working day periods that we studied.

The studied period include the two weeks previous to the declaration of the emergency state in Spain, and the four first weeks of lockdown, although the third and four weeks enter in the full lockdown period. We have chosen two representatives weeks of each period in order to have richer statistics when assessing the pollutant reductions in the lockdown situations.

4.3.1 Lockdown restrictions

In the BOE of 14^{th} March of 2020 [22], the Spanish government ordered an emergency rule that resulted in lockdown restrictions. Among other exceptional measures, this document included:

- Limitation to free movement of individuals. Circulation was restricted to a few justified cases such as food supply, medical emergencies or displacement to work place.
- Cease of educational activity.
- National public transport offer was lowed to 50%.
- Non-essential stores were forced close to the public.

In the BOE, the sectors and business considered essential include supermarkets and other food supply stores, pharmacies and other medical supply stores, technological shops (because of the imposing of tele-working) and hygienic services such as laundry.

This measures were toughened in the BOE of 28^{th} March of 2020 [23] due to the negative evolution of the COVID pandemic. In order to restrict more social contact and mobility, the Spanish government ordered the closure of all non-essential business, like offices which were still opened without customer service, and workers were ordered to stay home following the mobility restrictions already current.

The possible impact of this remarkable additional measure has to be considered. Therefore, we have to make a distinction between the two periods. We shall refer to the period including the first two weeks, 16^{th} March - 29^{th} March, as **lockdown** period. On the other hand, the period 30^{th} March - 10^{th} April shall be referred to as **full lockdown** period.

4.3.2 Meteorological conditions

When assessing air quality, one of the most important factors to consider is meteorology. Similar anthropological behavior and emissions can have a different impact on air quality depending on meteorological conditions. In general terms, unstable weather conditions such as windy and rainy episodes favor air cleansing and improve air quality. On the other hand, stable atmospheric conditions favor pollutant accumulation [25]. Moreover, there could be natural causes for bad air quality. For instance, there are dust storms coming from the Sahara desert that can reach and affect the air in Catalonia.

The meteorological conditions in the different stages of our study period are characterised by no extreme windy events, low solar irradiation and hot temperatures compared to previous years ([42], [43]). However, in March we find slight different weather conditions for the two studied periods (pre-covid time and first lockdown period). During the first fortnight of March 2020, the maximum absolute temperatures where reached in atmospherical stable days. In contrast, during second fortnight of the month a higher weather variability occurred with more rainy events and colder and less sunny days [42].

The meteorological phenomenons that can induce punctual changes in air quality are precipitation events. During the studies period there were five rain episodes in the 1^{st} - 3^{rd}, in the 15^{th} - 17^{th} March, 22^{nd} - 23^{rd} March, 25^{th} - 26^{th} March and finally the precipitations that occurred between the 29^{th} of March and the 2^{nd} of April. Despite having an irregular distribution, all these precipitation events effected the city of Barcelona and the AMB ([42], [43]). Though there were not intense rains, we expect to minimize possible particular effects of these and other phenomenons by averaging over a large period. In addition, another remarkable atmospheric event in terms of air quality assessing are the African dust episodes that affected Barcelona from the 28^{th} of February to the 1^{st} of March and from the 18^{th} March and lasted until the 24^{th} of the same month [42].

A summary of the meteorological conditions per weeks in the city of Barcelona is presented in Table 5. The table includes the studied week (only working days), the current restriction regime and the main meteorological variables. The data presented show the daily average during of week computed with data from the meteorological stations in Barcelona provided by the SMC (*Servei Meteorològic de Catalunya*). Alongside with the main meteorological variables, like pressure surface (P_{sfc}), temperature (T) and accumulated precipitation (Prec. acc.); Table 5 also gives insight on two larger-scale variables. In short, the circulation weather type (CTW) gives insight on the origin of the atmospheric circulation: cyclonic/anti-cyclonic, purely advective winds or the combination of both. On the other hand, the synoptic wind component (SWC) indicates the main direction of the wind.

4.3.3 Post-processing data for results

The results presented in this work can be classified within three categories.

- **Pollutant time series**. The evolution of a daily variable is computed and plotted in the whole study period. We do so for the 24h-mean and 8h-mean maximum of pollutant concentrations. To perform this calculation, we compute firstly the evolution of the chosen variable in each station. These time-series are then averaged over all the stations in the AMB.

Week	Description	P_{sfc} (hPa)	T(^{o}C)	Prec. acc. (mm)	CWTs	SWC
16th - 20th March	Lockdown	1020.4	12.9	24.1	SE	SE
23rd - 27th March	Lockdown	1015.8	11.4	20.4	E	E
30th March - 3rd April	Full lockdown	1015.9	11.6	25.3	C	E
6th - 10th April	Full lockdown	1023.0	15.0	0	A	S

Table 5: Weather conditions of the selected four weeks in Barcelona. P_{sfc}: surface pressure. *Prec. acc.*: precipitation accumulated (mm). *CWT*: circulation weather type. *SWC*: Synoptic Wind Component

The incertitude of this data has two error sources. On one side, there is an statistic deviation of the temporal data in each station. And on another side, there is an variation between the different stations.

In the case of the 8h-mean maximum, we follow this same procedure. But, once the AMB time series of the 8h-mean has been computed, we choose the maximum daily values.

- **Agregated daily profiles.** With this kind of plot we define an averaged daily behaviour of a pollutant concentration in a certain period.
  The first step of the calculation consists in perform the hourly data averages over all the AMB stations, or alternatively, the stations of one of the sectors we defined. When doing this calculation it has to be taken into account that XVPCA provides hours in local time (LT) and the model uses UTC time. So, the proper conversion has to be considered. During winter months (before the 28th March): LT is UTC + 1h. For summer months (after the 28th) LT is UTC + 2h.
  Then, with the second stage of this calculation, we find a generic daily profile of a pollutant concentration by computing the median of the different days of the studied period.
  To provide some insight on the variability of this data, we include in this plots the value of the percentiles.

- **Reduced concentration percent.** In order to quantify the reduction predicted by the model, we compute the percentage difference between the two simulation.
  This substraction is performed on every hourly value following the below expression, (1):
  $$\frac{x^j_{COVID} - x^j_{BAU}}{x^j_{BAU}} \times 100 \quad (1)$$
  where x^j_σ stands for the value of the variable in time j and for simulation σ.

5 Model evaluation

Previously to the discussion of the model simulated data and its comparison with observation data, we make a first assessment of the performance of the model. To do so, we take as a benchmark data of the first two weeks of March. This period correspond to the first fifteen simulated days and also it is previous to the lockdown imposition. Therefore,

in this period the model only simulates a BAU situation and we work only with one set of simulated data, BAU data, and with observation data provided by the XVPCA.

We evaluated three statistic metrics: the correlation coefficient, the root mean squared error and the normalized mean bias. In the following equations P and O shall denote the predictions data vector (modelled data) and observations data vector, respectively. Also, we keep the tradition nomenclature for statistic variables: $\bar{x}$ stands for mean and σ_x for standard deviation.

- Correlation coefficient (R). It provides a measure of the lineal relation intensity between two variables. But it does not contain insight on the their bias.

$$R = \frac{1}{N} \sum_{i=1}^{N} \frac{(O_i - \bar{O}) \cdot (P_i - \bar{P})}{\sigma_O \cdot \sigma_P} \tag{2}$$

- Root Mean Squared Error ($RMSE$). Statistical estimator that gives the mean error of two sets of data. For example, data provided by a predictive model and data got from an experiment.

$$RMSE = \sqrt{\frac{1}{N} \sum_{i=1}^{N} (P_i - O_i)^2} \tag{3}$$

- Normalized Mean Bias (NMB). Metric that quantifies the under or overestimation, depending on the sign of the observed mean by the predicted mean.

$$NMB(\%) = \frac{\sum_{i=1}^{N} (P_i - O_i)}{\sum_{i=1}^{N} O_i} \times 100 = \left(\frac{\bar{P}}{\bar{O}} - 1 \right) \times 100 \tag{4}$$

The calculation of these magnitudes has been done pollutant by pollutant and station by station. That is, for every station of each pollutant we take as O-vector the complete time series of data from the 1$^{\text{st}}$ of March at 00:00 h to the 15$^{\text{th}}$ of March at 23:00 h (hourly values). Analogously, the P-vector is build with the same time series of data taken from the BAU simulation output in the simulation grid point closest to the station location, which is given by a pair of coordinates: latitude, longitude.

Once the statistic metrics are computed for every station, we can get the mean values for each of the defined sectors. To do so, we average the results for all the stations of a certain sector. The statistic metrics computed for every pollutant on every sector are presented in Table 6.

From the results of our assessment we can conclude that, in general terms, the capacity of the model to simulate the behaviour of PM_{10} concentration is limited. The correlation coefficient values are below 0.3 and we get biases greater than 50%, in absolute value. To evaluate the $RMSE$ results, we compare them to the guideline level proposed by the WHO. Such value provides an idea of the order of magnitude of the concentration of a pollutant. In the case of PM_{10} we find root mean squared errors around 17 μg/m^3, which has the same order of magnitude of the annual mean WHO guideline, 20 μg/m^3. That is, the expected error has the same magnitude as the maximum expected value.

An analogous conclusion stands for the metrics found for CO. The values for R are low and the $RMSE$ has the same value as the typical levels of CO concentration. Although

we could confer these poor statistic metrics to the fact that for these two pollutants, CO and PM_{10}, are monitorized by a reduced number of stations in the AMB, 8 and 10 respectively.

On the other hand though, for NO and NO_2, which are monitorized by 20 stations in the AMB, we may expect more consistent results. The statistic metrics presented in Table 6 for these pollutants show larger values for the correlation coefficient and $RMSE$ that are one order of magnitude smaller than the WHO threshold levels. Also, for the case of NO_2 we got normalized mean biases below 50%. And, except for Urban - Traffic and Suburban - Traffic sectors for which there are only two stations monitoring NO_2, the biases found are below 30%.

For the case of ozone, despite being measured only in 13 stations in the AMB, the statistic metrics point to an acceptable agreement between observation data and the data computed by the model. The correlation coefficient take values around 0.7 in all cases and the root mean squared error varies in a close range and values are well below the level set by the WHO guideline ($100\,\mu g/m^3$).

Pollutant	Sector	Num. stations	R	$RMSE$	NMB
PM_{10}	AMB complete	10	0.1848	$17.869\,\mu g/m^3$	-52.35%
	Urban - Traffic	2	0.0357	$21.337\,\mu g/m^3$	-61.21%
	Suburban - Traffic	1	0.2322	$17.015\,\mu g/m^3$	-52.34%
	Urban - Background	4	0.1552	$18.066\,\mu g/m^3$	-52.78%
	Suburban - Background	2	0.3074	$15.902\,\mu g/m^3$	-44.79%
O_3	AMB complete	13	0.7016	$27.543\,\mu g/m^3$	36.75%
	Urban - Traffic	2	0.6994	$27.975\,\mu g/m^3$	43.94%
	Suburban - Traffic	1	0.7372	$37.024\,\mu g/m^3$	86.95%
	Urban - Background	5	0.7357	$26.636\,\mu g/m^3$	36.43%
	Suburban - Background	5	0.6613	$26.380\,\mu g/m^3$	24.17%
NO	AMB complete	20	0.4352	$18.234\,\mu g/m^3$	-46.31%
	Urban - Traffic	2	0.5881	$21.032\,\mu g/m^3$	-55.59%
	Suburban - Traffic	2	0.3599	$33.513\,\mu g/m^3$	-85.18%
	Urban - Background	9	0.4646	$17.221\,\mu g/m^3$	36.43%
	Suburban - Background	6	0.3770	$13.616\,\mu g/m^3$	-36.68%
NO_2	AMB complete	20	0.4788	$20.366\,\mu g/m^3$	-24.69%
	Urban - Traffic	2	0.5053	$24.878\,\mu g/m^3$	-38.50%
	Suburban - Traffic	2	0.3877	$23.504\,\mu g/m^3$	-44.49%
	Urban - Background	9	0.5164	$20.693\,\mu g/m^3$	-27.10%
	Suburban - Background	6	0.4499	$17.335\,\mu g/m^3$	-5.59%
CO	AMB complete	8	0.2203	$0.21\,mg/m^3$	-54.52%
	Urban - Traffic	2	0.1376	$0.256\,mg/m^3$	-54.38%
	Suburban - Traffic	1	0.1659	$0.125\,mg/m^3$	-38.45%
	Urban - Background	2	0.2390	$0.186\,mg/m^3$	-48.74%
	Suburban - Background	3	0.2809	$0.259\,mg/m^3$	-63.81%

Table 6: Statistic metrics for model evaluation. For each pollutant, the computation has been done for sectors.

As an exception we have to remark the results found for the Suburban - Traffic sector. This sector is only represented by a single station for ozone and therefore, possible local variations are not mitigated by the average behaviour of several stations.

One reason for these good results of ozone respect the other pollutants might be its behaviour in the atmosphere. Unlike NO_x, CO and PM_s, ozone is not directly emitted but it is created and destroyed by a complex chain of chemical reactions in the atmosphere. Then, while primary pollutants (NO_x, CO, PM_s) are deeply affected by the emissions used as boundary conditions for the model, ozone is not. It has to be remind here that the emission set used for the execution of the model correspond to the emissions of year 2016. So, here there is one of the error sources of the model.

6 Results and Discussion

In this section we discuss every chosen pollutant, PM_{10} and O_3, separately. For each pollutant we discuss whether the model is capable of capture the evolution of the observational data in the studied period, as well as the daily trends of the concentration levels in the AMB. This qualitative discussion is later combined with a quantification of the pollutant concentration reductions computed with modelled data. In addition, we perform sectoral discussion of the results analyzing the aggregated daily profiles of each defined sector and we quantify the model reductions.

Furthermore, for ozone we include a deeper discussion taking into account its chemical process in the atmosphere. To this end, we perform a briefer analysis of the model results on the principal pollutants that influence ozone chemical cycle: NO, CO and NO_2.

6.1 PM_{10} analysis

As our model performance assessment pointed (section 5), the general behaviour of PM_{10} is not captured by the model. For instance, in Figure 4 we see how the model shows concentration peaks where the XVPCA register off-peaks as it is the case of the peak that is appreciated on March 16^{th} and, to a less extend, the peak simulated on April 4^{th}.

Another example of this lack of agreement between the model and the simulation is found in the trend simulated between the 24^{th} - 28^{th} of March: the XVPCA register a decrease in the levels of pollutant whereas the model points to a PM_{10} concentration increase.

In addition, the concentration levels are sub-estimated in pre-covid and lockdown (lockdown and full-lockdown) periods. As it is seen in Figure 4, even for the reduced levels of PM_{10} that occur during the restrictive period, the prediction of the model is well below the observations data. This same analysis can be derived from the aggregated daily profile of PM_{10} concentration in the AMB, Figure 5.

The model results do not show major differences between the two simulations. In both, Figure 4 and 5 the COVID and BAU lines follow the same trends and take similar values. In fact, the variations computed from modeled data show an slight decrease of 0.65% during the lockdown period and an slight increase of 5.18% in the full lockdown period. In general, the variation between both simulations for the PM_{10} concentration in the

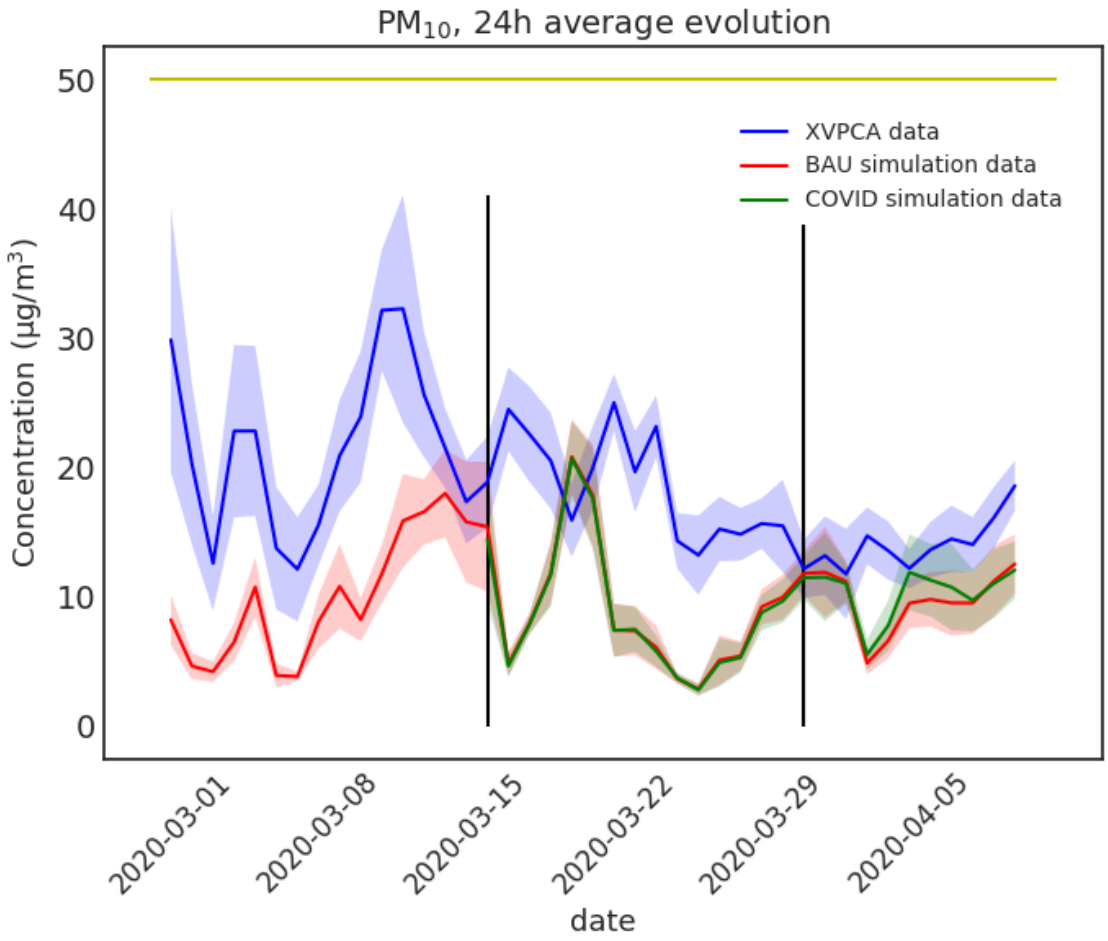

Figure 4: Evolution of the PM_{10} concentration 24h-mean in the studied periods: from 1^{st} of March to the 10^{th} of April. The black vertical lines mark the change of restrictive perdios: pre-covid, lockdown and full lockdown. The horizontal yellow line sets the WHO threshold level for the PM_{10} 24h-mean: $50\mu g/m^3$

.

AMB is +1.64% (where a positive sign means an concentration increase).

In respect to the observational data, it is well appreciated how the pollutant concentration decreases in time due to the application of mobility restrictions (Figure 4). In particular, we highlight the smoothing and reduction of the morning peak that is seen in the Pre-covid panel of Figure 5. This peak is almost undetectable in the last panel of this same figure.

A sectoral analysis of this pollutant show that, for traffic stations (Figure 6 panels *(a)* and *(b)*), the pollution levels are greater than for background stations (Figure 6 panels *(c)* and *(d)*). Also, the relative reduction is greater for traffic stations so in the full-lockdown period the levels of PM_{10} are equal for all sectors. When comparing the aggregated daily profiles of the PM_{10} concentration (Figures 5, 6), it is seen that the morning peak is mainly due to traffic pollution: for traffic stations this peak can reach concentrations of $70\mu g/m^3$, while in background stations it hardly exceed a $30\mu g/m^3$ value.

In terms of model results, the computed variations for sectors are around +2% for all

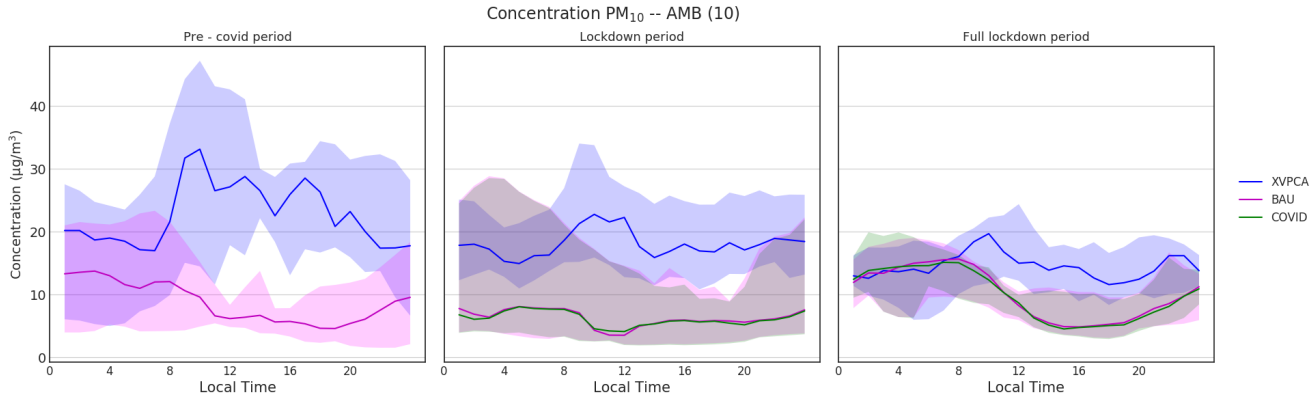

Figure 5: Aggregated daily profiles of all the stations monitoring PM_{10} in the AMB. **Precovid period** (left panel): aggregated profile for working weeks: 2nd March - 6th March and 9th March - 13th March. **Lockdown period** (middle panel): aggregated profile for working weeks: 16th March - 20th March and 23rd March - 27th March. **Full-lockdown period** (right panel): aggregated profile for working weeks: 30th March - 3rd April and 6th April - 10th April.

sectors. Specifically, +1.04% for Urban - Traffic stations, +1.64% for Urban - Background stations, +2.64% for Suburban - Traffic station and +2.24% for Suburban - Background stations.

This increase in PM_{10} levels contrasts with the 21% PM_{10} reduction observed in Barcelona [5]. It seems that the model does not translate an emission reduction in a PM_{10} reduction. We recall here that the emission set used in the COVID situation is defined using the reduction factors presented in [41]. According to this work, PM_{10} emission increase for the *Other Stationary Combustion* sector, see Figure 3 in Section 4.1.3. So, we could attribute the increase in simulated PM_{10} levels to an over-estimation of these emissions.

6.2 Ozone chemistry: analysis of NO, NO_2 and CO

In this section we analyze the results of the model for three pollutants that, as we explained in section 3.2, may have an effect on ozone chemical processes. For each of these three pollutants, we present first an overall discussion of the agreement between modelled data and observational data. Then analyze only modelled results and quantify the pollutant concentration variation. Finally, at the end of this section, we will discuss the what might be the effect of this variation on the variation in ozone levels.

6.2.1 Analysis of NO

For nitrogen monoxide, the model gets the actual trends of its concentration, see Figure 7. However, we see a remarkable under-estimation of the NO levels, specially of its concentration peaks. This inaccuracy of the model is manifested more clearly in the aggregated daily profiles, where it is clearly seen that the morning NO peak is much greater than the simulated value, see Figure 8. The presence of this peak is not particular of an specific type of stations, but it occurs in all four defined sectors. Nevertheless, it takes higher values for Traffic stations, where the maximum exceeds $100\mu g/m^3$, than for

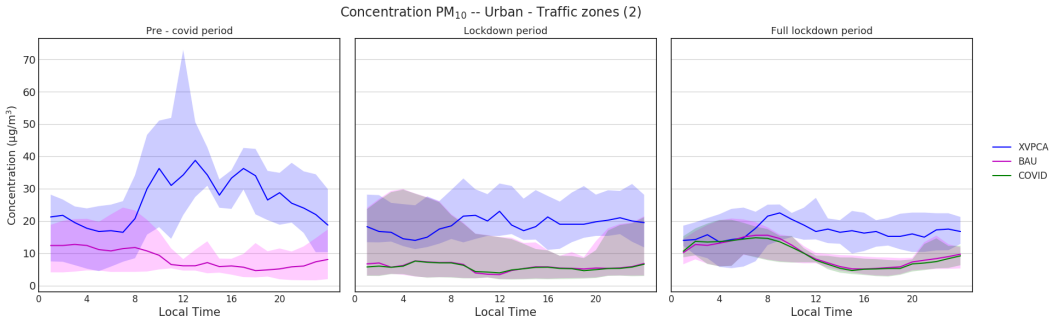

(a)

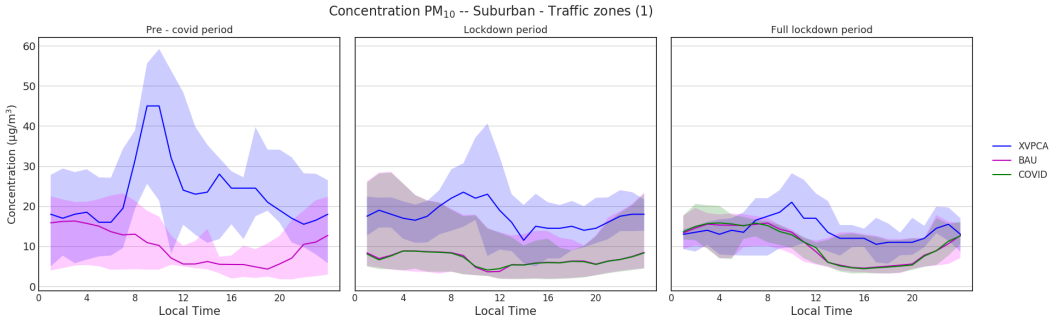

(b)

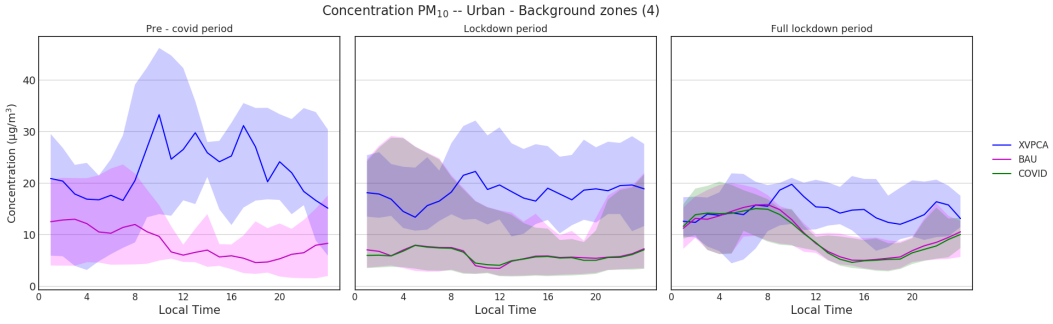

(c)

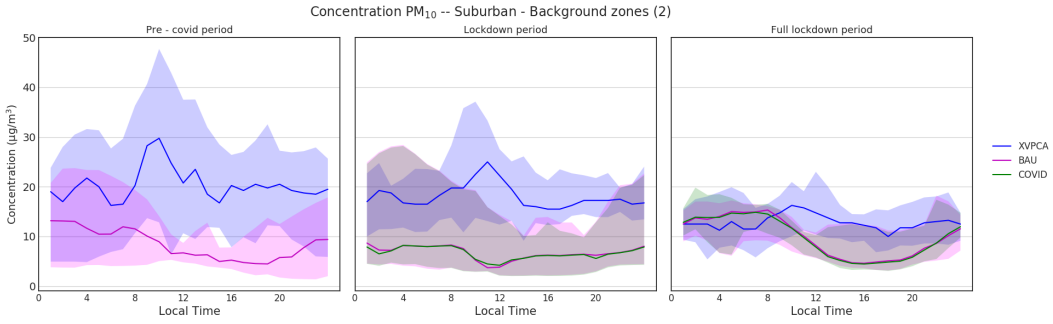

(d)

Figure 6: PM_{10} aggregated daily profiles for each sector. *(a)* Traffic - Urban stations. *(b)* Traffic - Suburban stations. *(c)* Background - Urban stations. *(d)* Background - Suburban stations. The days used to compute the aggregated profile of each period are the same described in Figure 5.

Background stations, where it is kept below $80\mu g/m^3$.

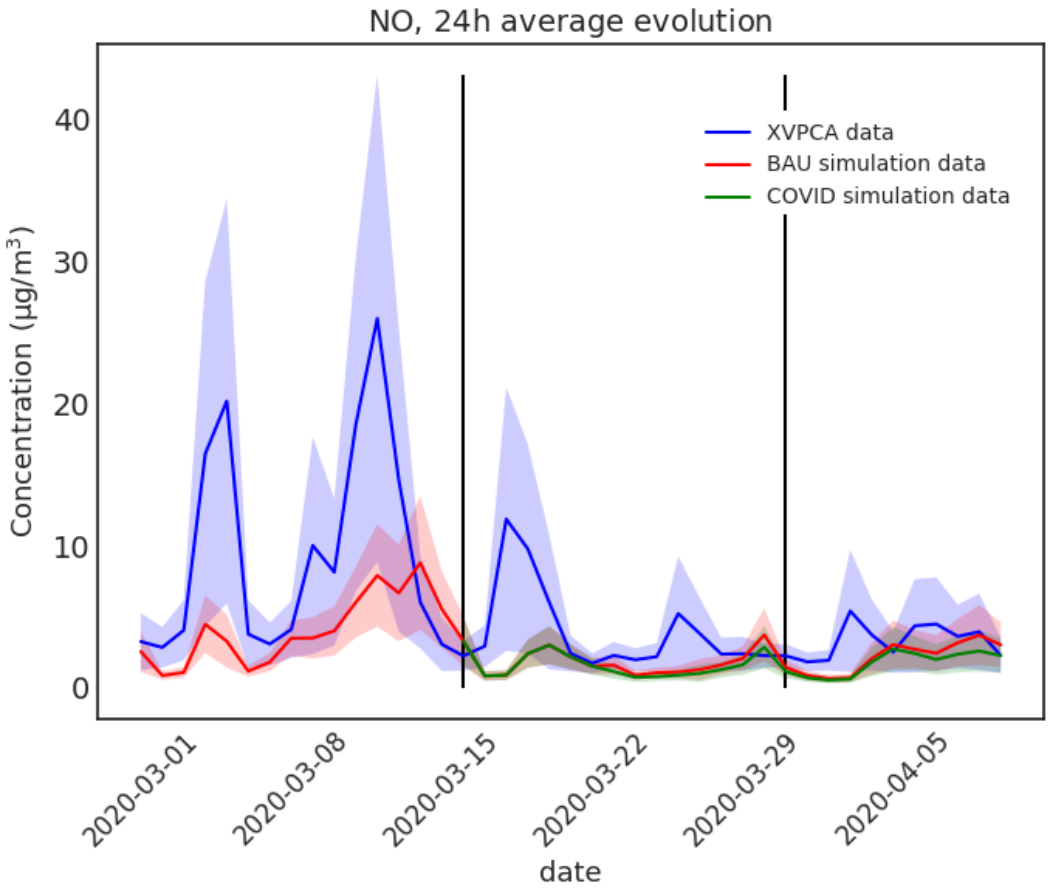

Figure 7: Evolution of the 24h-mean of NO concentration in the studied period: from 1st of March to the 10th of April. The black vertical lines mark the change of restrictive periods: pre-covid, lockdown and full lockdown. We do not include the WHO threshold line since it is not defined for NO daily mean.

This peak underestimation is smoothed in lockdown periods mainly due to an important reduction of the observed levels of NO. It is seen in Figure 8 that the morning peak is reduced from concentrations around $100\mu g/m^3$ in pre-covid times to levels below $20\mu g/m^3$ in the full-lockdown period. In any case, though, it can be said that the model presents a better performance in this latest period. Figures 7 and 8 indeed point to a reduction of NO levels when emissions are reduced (lockdown periods) but it is not as pronounced as the one observed. The simulated morning peak is reduced from $20\mu g/m^3$ to around $10\mu g/m^3$.

Having said that, analyzing only modelled data, we find that the model predicts a NO reduction when comparing BAU and COVID simulations. Moreover, this reduction becomes more noticeable when restrictions are toughened. The computed reduction during the first lockdown period is -12.54% and during full-lockdown days NO concentration is reduced in a -20.10%.

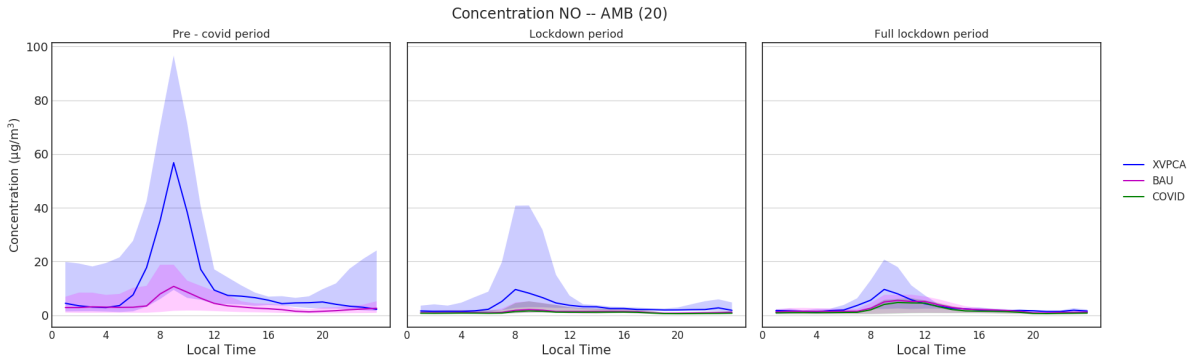

Figure 8: Aggregated daily profiles of all the stations monitoring NO in the AMB. **Pre-covid period** (left panel): aggregated profile for working weeks: 2nd March - 6th March and 9th March - 13th March. **Lockdown period** (middle panel): aggregated profile for working weeks: 16th March - 20th March and 23rd March - 27th March. **Full-lockdown period** (right panel): aggregated profile for working weeks: 30th March - 3rd April and 6th April - 10th April.

6.2.2 Analysis of NO_2

As in the case of NO, NO_2 levels during pre - covid days are under-estimated but to a lesser extend. Also, we can see that the evolution trends are captured by the model and how both concentrations, modelled and observed, are reduced in every period. See Figure 9.

The daily trend is also captured with a significant temporal shift. In Figure 10 we see how NO_2 presents two peaks during the day, one in the morning and another one in the first hours of the night. While the usual time between peaks is of 11 hours, the model predicts a larger time for all periods. The morning peak appears one hour early and the second peak, one hour later. As it happened for NO morning peaks, both NO_2 peaks are smoothed when restrictions are applied for both observed and modelled data.
This behaviour is seen in all four sectors. And, as it is in the case of nitrogen monoxide, the concentration levels in Traffic stations are greater than for Background stations.

The differences between the COVID and BAU simulation result in a reduction of NO_2 concentration for the COVID simulation. Such reduction becomes clearer when full-lockdown restrictions are applied. The averaged reductions go from -9.33% in lockdown period to -16.59% in full-lockdown period. Observed data also shows a reduction in NO_2 levels, though it is significantly larger: 50% average reduction in AMB stations [25].

6.2.3 Analysis of CO

In the case of carbon monoxide we can not recognize the same evolution pattern in observed data and in modelled data, see Figure 11. In the pre-covid period, the model under-estimates the CO concentration whereas in the first lockdown period CO levels drop with restriction implementation while the modelled do not, leading to an over-estimation of CO concentration.

Furthermore, in Figure 11 we see on the one hand that the observed CO stabilises in the full-lockdown period. And on the other hand, we can see how the simulated CO

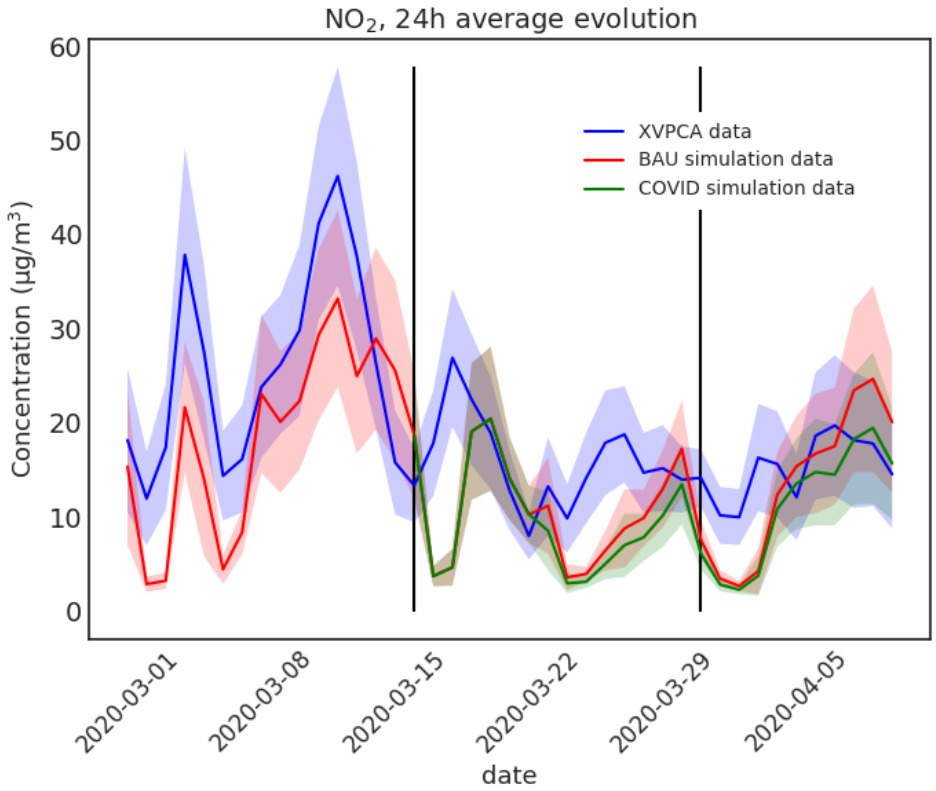

Figure 9: Evolution of the 24h-mean of NO_2 concentration in the studied period: from 1st of March to the 10th of April. The black vertical lines mark the change of restrictive periods: pre-covid, lockdown and full lockdown. We do not include the WHO threshold since it is not defined for NO_2 daily mean.

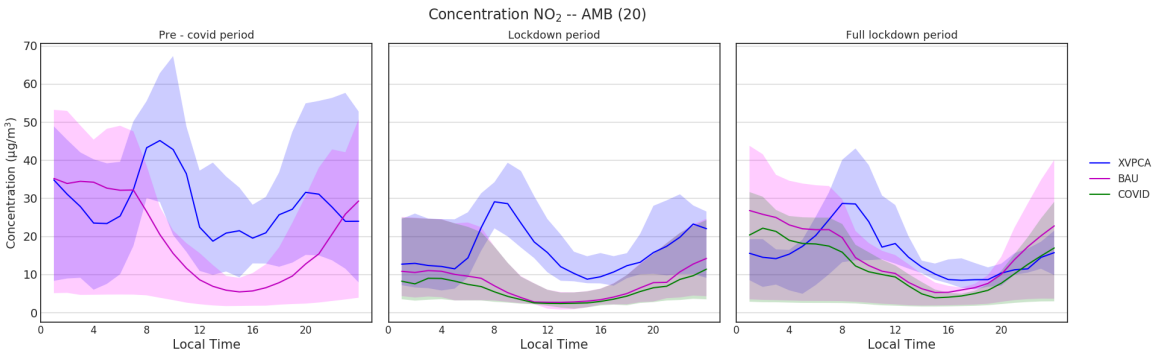

Figure 10: Aggregated daily profiles of all the stations monitoring NO_2 in the AMB. **Precovid period** (left panel): aggregated profile for working weeks: 2nd March - 6th March and 9th March - 13th March. **Lockdown period** (middle panel): aggregated profile for working weeks: 16th March - 20th March and 23rd March - 27th March. **Full-lockdown period** (right panel): aggregated profile for working weeks: 30th March - 3rd April and 6th April - 10th April.

concentration in the COVID simulation increases while it drops in the BAU simulation. An analogous discussion stands for the analysis of the aggregated CO profile, see Figure

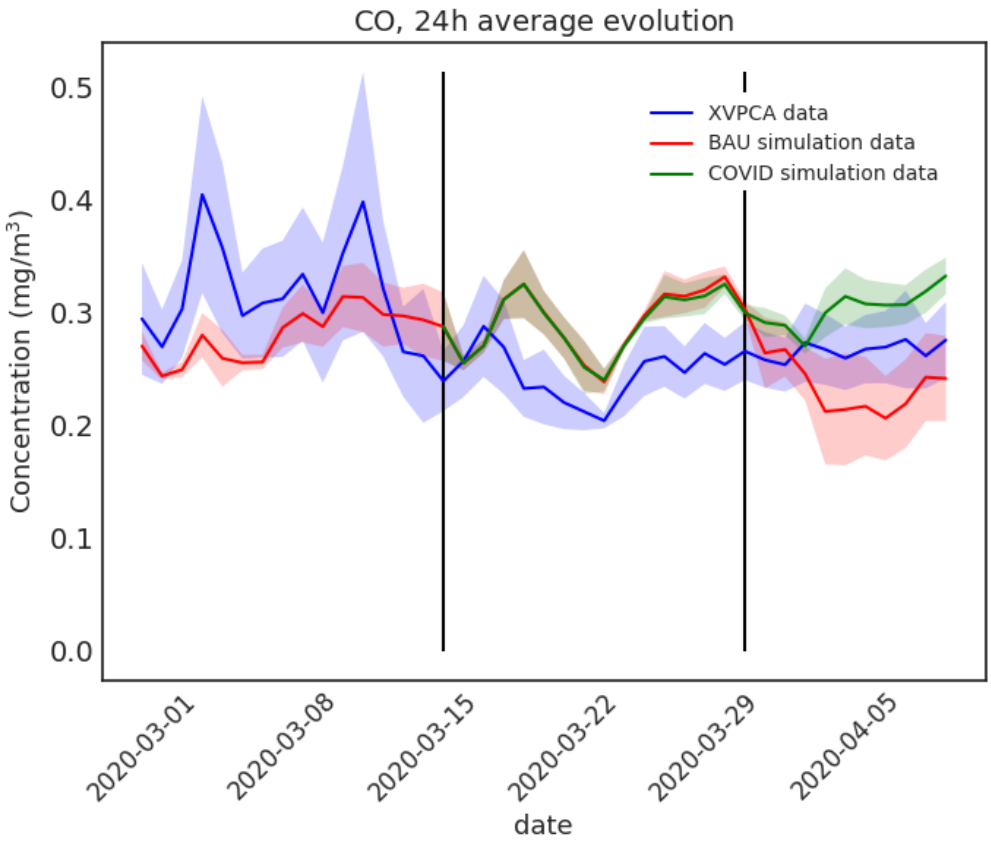

Figure 11: Evolution of the 24h-mean of CO concentration in the studied period: from 1st of March to the 10th of April. The black vertical lines mark the change of restrictive periods: pre-covid, lockdown and full lockdown. We do not include the WHO threshold line since it is not defined for CO daily mean.

12. In this case, though, we can also notice that the model does not capture the CO concentration morning peak, which suffers successive reductions in lockdown periods. All in all, the insight provided by Figure 12 reinforce the idea that there is not a recognizable evolution pattern between the model and the observed data.

In terms of air quality assessment, the WHO defines a guideline level of 10 mg/m^3 for the 8h-average maximum [21]. This threshold is not exceeded in any station neither by observational data or by modelled data. In fact, in the pre-covid stage, the CO morning peak (maximum value registered in a business as usual situation) does not exceed even a concentration of 1 mg/m^3.

Having said that, the simulated CO evolution presents an interesting behaviour. Carbon monoxide concentration in COVID-simulation conditions suffers a significant increase in opposition to the obvious reduction it suffers in BAU conditions. In fact, CO concentration in this last period increased in a 64.54% respect to BAU levels.

Due to this discrepancy between modelled and observed evolution, finding a relation between CO evolution and O_3 concentration becomes challenging. To do so, a deeper analysis on CO trends and chemistry would be required. However, this is beyond the scope of this project and therefore we shall proceed without taking into account the

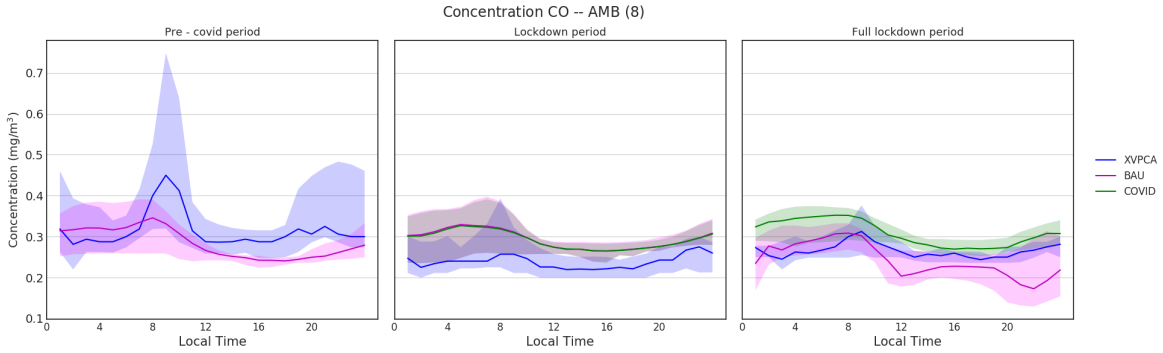

Figure 12: Aggregated daily profiles of all the stations monitoring CO in the AMB. **Precovid period** (left panel): aggregated profile for working weeks: 2nd March - 6th March and 9th March - 13th March. **Lockdown period** (middle panel): aggregated profile for working weeks: 16th March - 20th March and 23rd March - 27th March. **Full-lockdown period** (right panel): aggregated profile for working weeks: 30th March - 3rd April and 6th April - 10th April.

effect of CO on ozone in our subsequent analysis.

6.3 O_3 analysis.

Unlike the case of PM_{10}, the model gets correctly the trends of ozone in the whole study period, although it overestimates its concentrations. The ozone levels simulated by the model exceed the WHO threshold more frequently than the observed levels, see Figure 13. And, therefore, the model pictures a worse scenario in terms of air quality.

For the sake of simplicity, we shall proceed with our ozone results discussion with the evolution of its 24h-mean. Although this magnitude is not representative in terms of air quality assessment, it has less variability and therefore it enables an easier and more consistent analysis. See Figure 14.

In Figure 14 we can see how, despite a concentration overestimation, the overall behaviour of ozone is properly captured by the model. In addition, both the XVPCA data and the model prediction point to an increase in ozone concentration levels. In Figures 13 and 14, it can be seen how the COVID green line goes over the BAU red line, specially in the full lockdown period, and also how the blue line, which represents the evolution of the observations, reaches higher concentration levels during the lockdown periods.

A similar analysis stands for ozone aggregated daily profiles, see Figure 15. O_3 levels are over estimated and an increase in ozone levels is seen. Specifically, the computed variations of ozone are +0.41% in the first lockdown period and it reaches a +3.58% in the full-lockdown period. We see also how observed concentration grow in lockdown periods. In fact, we can this growth is even more significant than the given by the model, since in the Full-lockdown panel in Figure 15 the model over-estimation of ozone levels is hardly noticeable.

In addition, the daily behaviour of ozone is properly modelled: ozone concentration drops during night hours while suffering significant increases during daylight hours. This behaviour is due to the photo-chemical cycle of ozone in the atmosphere: ozone is produced

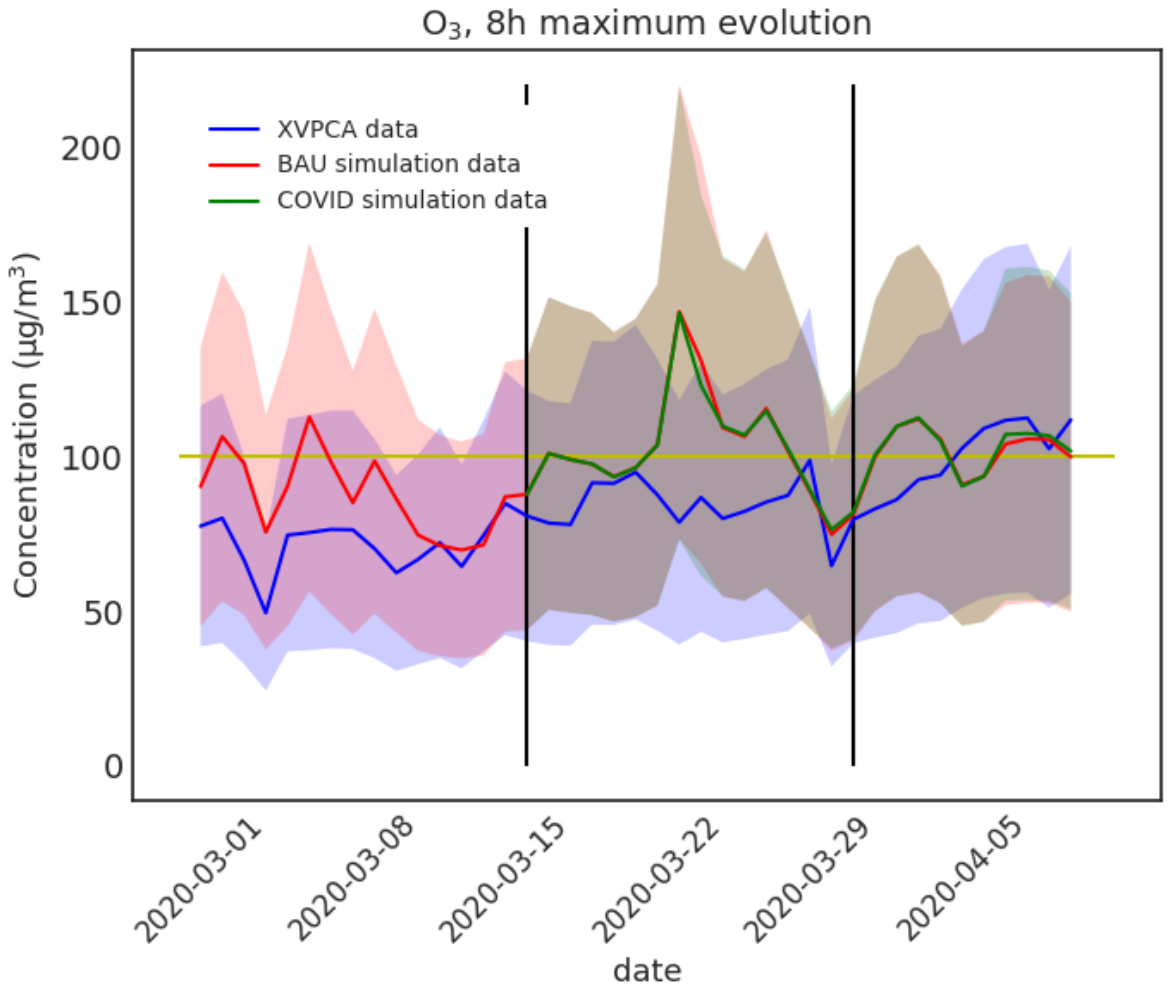

Figure 13: Evolution of the 8h-mean maximum of ozone concentration in the studied period: from 1st of March to the 10th of April. The black vertical lines mark the change of restrictive periods: pre-covid, lockdown and full lockdown. The horizontal yellow line sets the WHO threshold level for the O_3 8h-mean-maximum: $100\mu g/m^3$

by a complex chemical process, involving NO_2, NO, CO and VOCs, that requires sunlight, see Figure 1.

This agreement is extended to the results of all sectors. Specifically, for Background zones (Figure 16 panels *(c)* and *(d)*) which are monitored by 5 stations each (both, urban and suburban areas). For Traffic zones though, XVPCA data present more pronounced differences between day values and night values, see Figure 16 panels *(a)* and *(b)*. Since there are fewer traffic stations, we can consider these differences as a local behaviour undetected by the model.

In terms of ozone variations for sectors, differences between Urban and Suburban areas are remarkable. The averaged variations for Urban - Traffic and Urban - Background areas are +2.94% and 2.04% respectively, even reaching an increase of +6.14% in Urban - Traffic areas during the full lockdown period. On the other hand, variations in Suburban areas were more moderated. Ozone increases in a +1.03% in Suburban - Traffic stations

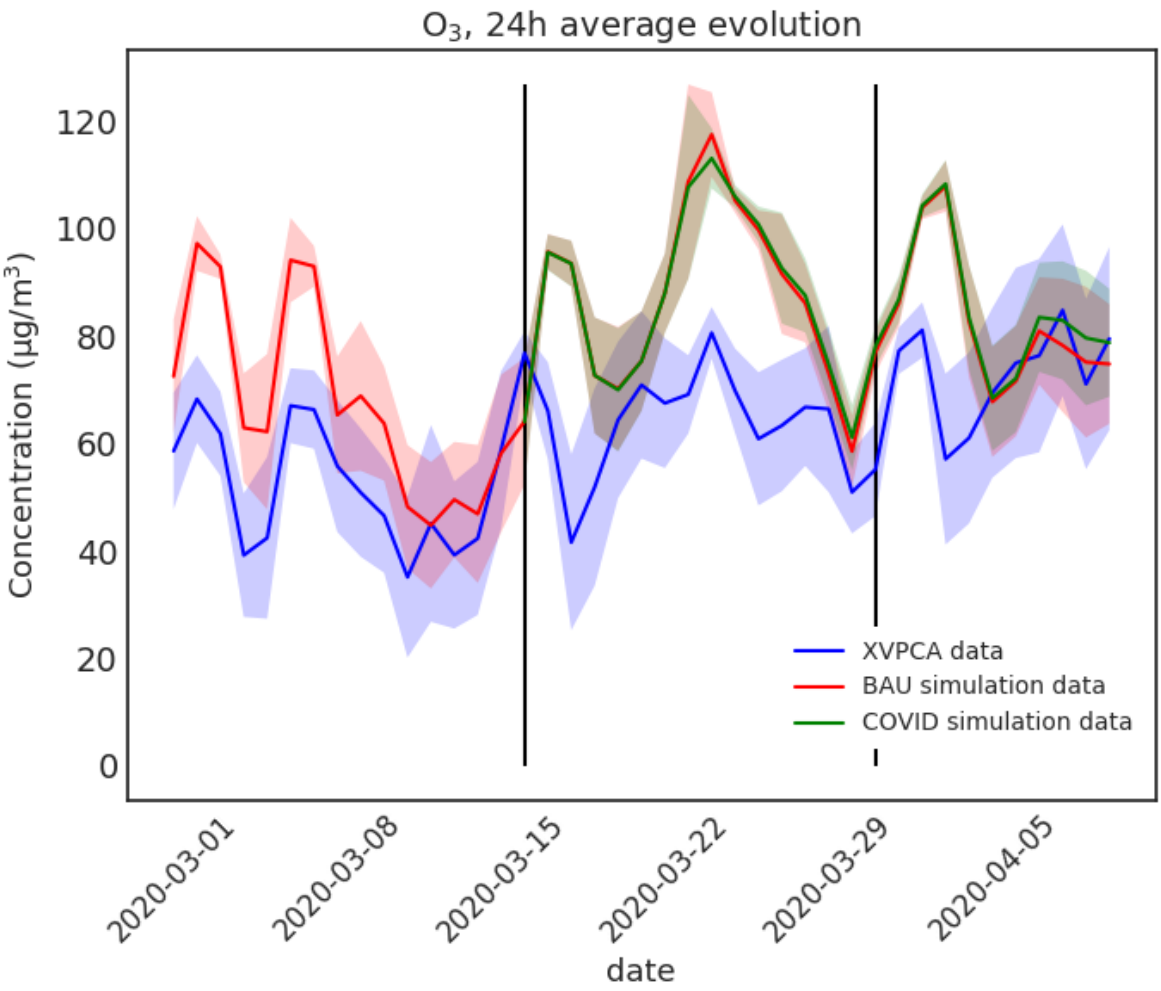

Figure 14: Evolution of the 24h-mean of ozone concentration in the studied period: from 1st of March to the 10th of April. The black vertical lines mark the change of restrictive periods: pre-covid, lockdown and full lockdown. We do not include the WHO threshold line since it is not defined for ozone daily mean.

and in a +1.31% in Suburban - Background stations, according to model results.

Observed data in Barcelona also shows significant increases in ozone levels in both traffic (+57.7%) and background stations (+28.8%) respect to the pre-covid period [5]. This phenomenology is not exclusive of Barcelona, but ozone concentrations increases have occured in the main urban areas in Spain [44] and has also been detected in Indian and Chinese cities ([4], [6]).

As it is has been discussed in [6] and following section 3.2, this increase in ozone concentration can be attributed to NO and NO_2 emissions reduction. Lower NO_x concentrations make ozone tritation more inefficient, that is ozone disappears slowly, and ultimately it results in higher ozone concentrations. It could be seen as a large-scale "weekend effect": increase of ozone during the weekend due to traffic emissions reduction [36]. Furthermore, in [4] it is speculated that a decrease in PMs can result in a reduced sunlight absorption and therefore in an increase in photo-chemical activities which lead to higher ozone

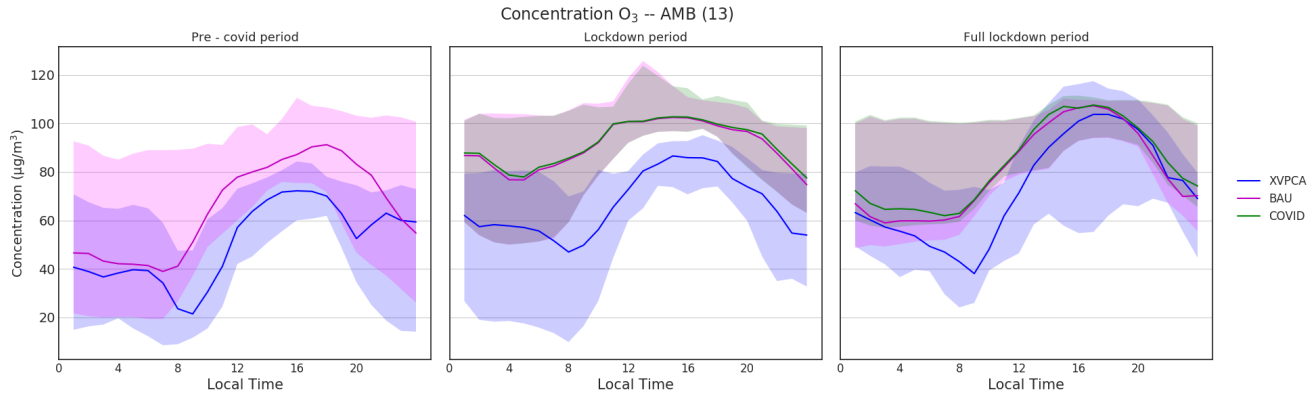

Figure 15: Aggregated daily profiles of all the stations monitoring O_3 in the AMB. **Precovid period** (left panel): aggregated profile for working weeks: 2nd March - 6th March and 9th March - 13th March. **Lockdown period** (middle panel): aggregated profile for working weeks: 16th March - 20th March and 23rd March - 27th March. **Full-lockdown period** (right panel): aggregated profile for working weeks: 30th March - 3rd April and 6th April - 10th April.

production.

7 Conclusions

As a general trend, the simulations generated by URBAG group underestimate the concentration levels of the primary pollutants (PM_{10}, NO, NO_2, CO) in the pre-covid period. That is, when there is no emission reduction. Part of this discrepancy could be due to the fact that XVPCA stations are strategically placed next to pollution hot-spots. Therefore, these stations are exposed to the highest concentration levels in a region. On the other hand, the emissions in the model are generally defined. So, concentration levels in the simulations are not that subjected to the particular behaviour of a pollution hot-spot.

Such behavior can be seen in the panels of Figure 6, showing the PM_{10} aggregated daily profiles for different sectors. The simulation lines show the same behaviour for all sectors. Simulated evolution present more stable variations (shadowed-areas), without abrupt changes or distinctive characteristics between different sectors except for slightly higher concentrations in Traffic stations. On the other hand, in the observed evolution we can identify differences between different sectors like a higher and clearer concentration peak in Traffic stations and significantly lower concentration levels in Background stations.

In contrast, ozone levels are overestimated by the model. Since it is a secondary pollutant, finding a cause for this discrepancy is not straightforward. To do so, we would have to study other chemical agents that can effect ozone production like VOCs. In this project though, we did not consider including VOC since we do not dispose of enough measures in the AMB to perform a proper analysis. On the other hand, in order to detect the source of this discrepancy we could gain deeper insight on which are the chemical processes considered and implemented in the model.

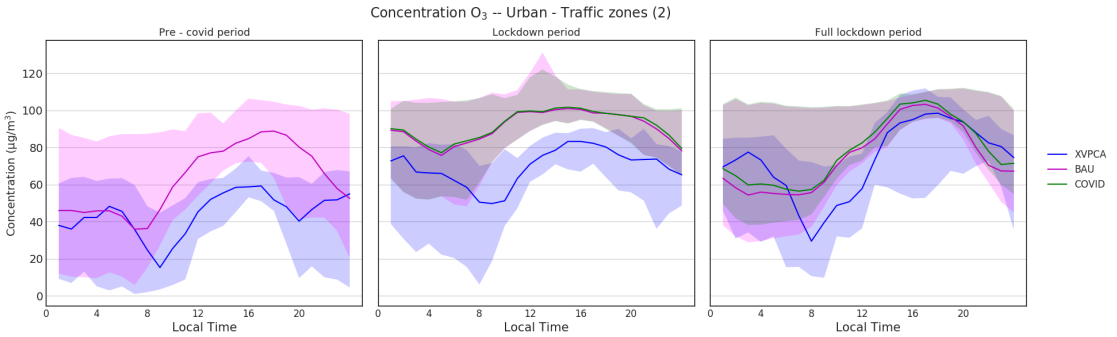

(a)

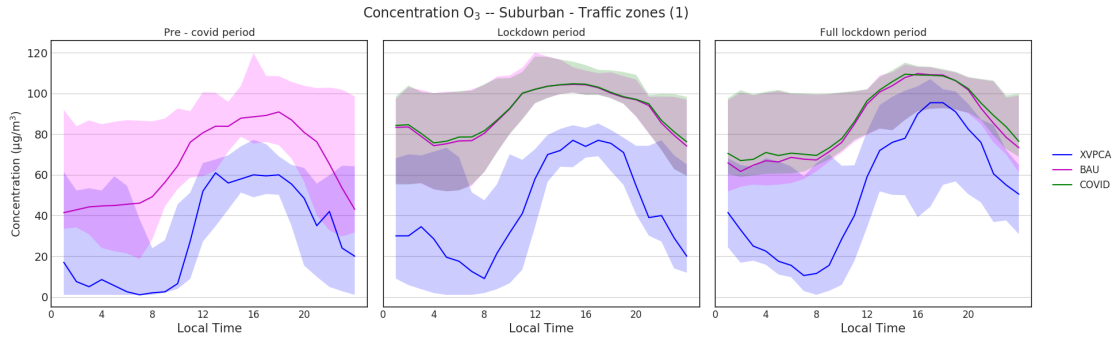

(b)

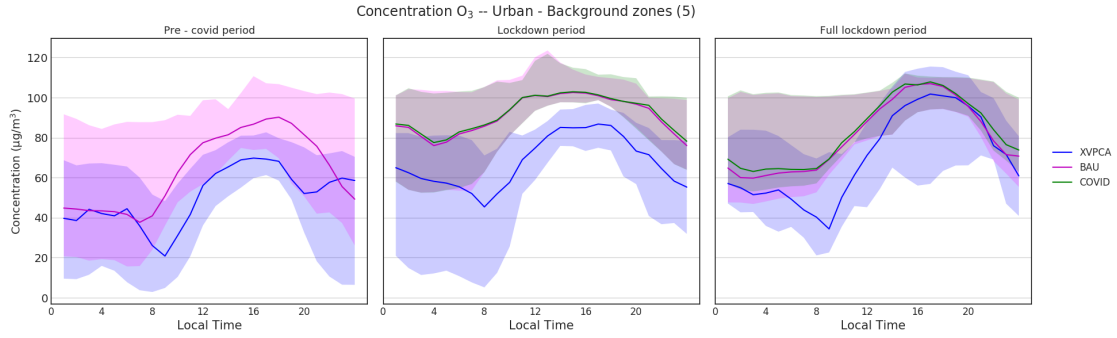

(c)

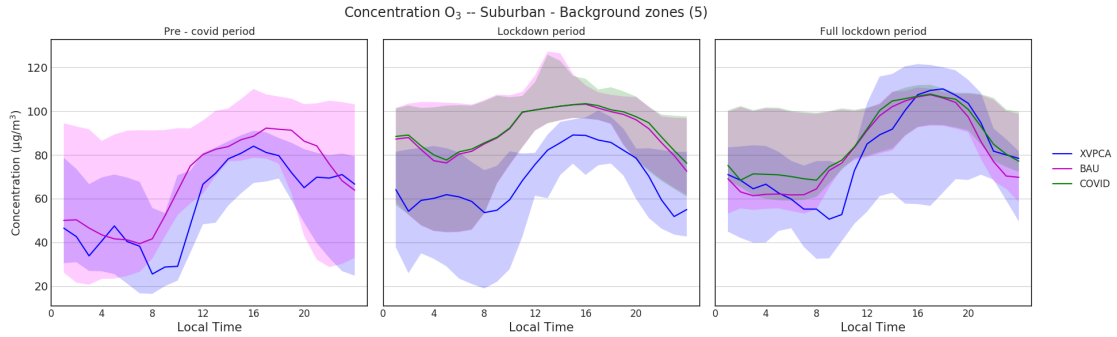

(d)

Figure 16: O_3 aggregated daily profiles for each sector. *(a)* Traffic - Urban stations. *(b)* Traffic - Suburban stations. *(c)* Background - Urban stations. *(d)* Background - Suburban stations. The days used to compute the aggregated profile of each period are the same described in Figure 15.

Besides these initial comments and assumptions on the differences between the modelled and observed data, we have to remark that a major discrepancy source in the models inputs (sec 4.1.2). First of all, the emissions used have been dis-aggregated from the CAMS-REG-APv3.1 data-set [39], which is an annual emission inventory with 2016 data. This procedure can introduce a non contemptible incertitude on NO and NO_2 concentrations as their principal sources are antrophogenic emissions. On the other hand, chemical boundary conditions [38] may affect long-living pollutants such as O_3 and CO as it is discussed in [45].

Regarding the differences between BAU and COVID simulations the model points to a significant decrease of NO (-15.87%) and NO_2 (-12.53%) concentrations while presenting slight increases in PM_{10} (+1.84%) and O_3 (+1.81%) levels. [5] Also, according to the model the most affected sector by the emission reduction effect for each pollutant are: suburban-traffic for NO (-23.67%), suburban-background for NO_2 (-19.36%) and PM_{10} (+6.68%) and urban-traffic for O_3 (+6.15%).

These results are far from the results provided by Tobías et al. [5]. According to their calculations, during the first lockdown period variations of -31% (PM_{10}), -51.0% (NO_2) and +57.7% (O_3) were registered in traffic stations respect to the previous two weeks (pre-covid period). Similarly for background stations they found variations of -27% (PM_{10}), -47.0% (NO_2) and +28.8% (O_3).

Despite the computation of these variations has been done differently to our computation, we can say that the model underestimates the effect of emission reductions leading to smaller variations and ultimately, to present a slight increase in PM_{10} levels. Such unexpected result can be related with the increase in PM_{10} emissions proposed in [41] for *Other Stationary Combustion* sources, see Figure 3.

A better analysis of the simulated data could have been performed taking into account more grid points within the AMB. These would provided us a better view of the overall situation in the region and made our statistics richer. However, we would had to face the challenge of classifying each of these grid points in one of the defined sectors. In addition, the comparison to observed data would not have been straightforward.

All in all, we can conclude that our methodology has its pros and cons. On the one hand, the choice of the simulation grid closest to a station enables us to identify the pollutant sector and also to compare the modelled data and observed data in a straightforward manner. On the other hand, statistics are poorer for some sectors like Suburban - Traffic since it is monitored only by one or two stations, depending on the pollutant (see Table 3). Also, our analysis is more subjected to possible anomalies that may effect one station but not the entire sector.

The results of our work open the door to new project proposals. For instance, an evaluation of the meteorological conditions simulated by the model could be performed. Such analysis would provide us more insight on possible discrepancies between the modelled results and observational data since meteorology is a key factor in air quality, as it has been discussed in section 4.3.2. For instance, possible study line would go through a further analysis of ozone chemistry. In this sense, other ozone precursors like VOCs could be included and a deeper discussion of the CO results and its role in ozone chemical

[5] These results correspond to the averaged variations in the whole lockdown period, including full lockdown period and on the whole AMB.

processes would have to be done. Moreover, to complete such analysis, the effect of boundary conditions on long-living pollutants should be a also evaluated. Furthermore, an important

References

[1] John Hopkins University, 2020. COVID-19 Dashboard by the Center for Systems Science and Engineering (CSSE) at Johns Hopkins University (JHU). `https://coronavirus.jhu.edu/map.html`, 2021

[2] Google LLC, 2020. Google COVID-19 community mobility reports. Available online at `https://www.google.com/covid19/mobility`.

[3] Rodríguez-Urrego, Daniella, and Leonardo Rodríguez-Urrego. "Air quality during the COVID-19: PM2.5 analysis in the 50 most polluted capital cities in the world." *Environmental pollution* (Barking, Essex : 1987) vol. 266,Pt 1 (2020): 115042. doi:10.1016/j.envpol.2020.115042

[4] Sharma, Shubham et al, 2020. "Effect of restricted emissions during COVID-19 on air quality in India." *The Science of the total environment* vol. 728 (2020): 138878. doi:10.1016/j.scitotenv.2020.138878

[5] Tobías, Aurelio et al. "Changes in air quality during the lockdown in Barcelona (Spain) one month into the SARS-CoV-2 epidemic." *The Science of the total environment* vol. 726 (2020): 138540. doi:10.1016/j.scitotenv.2020.138540

[6] Le, Tianhao et al. "Unexpected air pollution with marked emission reductions during the COVID-19 outbreak in China." *Science (New York, N.Y.)* vol. 369,6504 (2020): 702-706. doi:10.1126/science.abb7431

[7] Cohen, Aaron J et al. "Estimates and 25-year trends of the global burden of disease attributable to ambient air pollution: an analysis of data from the Global Burden of Diseases Study 2015." *Lancet (London, England)* vol. 389,10082 (2017): 1907-1918. doi:10.1016/S0140-6736(17)30505-6

[8] Coccia, Mario. "Factors determining the diffusion of COVID-19 and suggested strategy to prevent future accelerated viral infectivity similar to COVID." *The Science of the total environment* vol. 729 (2020): 138474. doi:10.1016/j.scitotenv.2020.138474

[9] Zhu, Yongjian et al. "Association between short-term exposure to air pollution and COVID-19 infection: Evidence from China." vol. 727 (2020): 138704. doi:10.1016/j.scitotenv.2020.138704

[10] Kayalar, Özgecan et al. "Existence of SARS-CoV-2 RNA on ambient particulate matter samples: A nationwide study in Turkey." *The Science of the total environment* vol. 789 (2021): 147976. doi:10.1016/j.scitotenv.2021.147976

[11] Cimorelli, A. et al. (2005). "AERMOD: A Dispersion Model for Industrial Source Applications. Part I: General Model Formulation and Boundary Layer Characterization." *Journal of Applied Meteorology - J APPL METEOROL.* 44 (2005). doi:10.1175/JAM2227.1.

[12] Menut, L., et al. "The CHIMERE v2020r1 online chemistry-transport model." *Geoscientific Model Development Discussions* (2021): 1-50.

[13] Basart, S. et al. "Development and evaluation of the BSC-DREAM8b dust regional model over Northern Africa, the Mediterranean and the Middle East." *Tellus B: Chemical and Physical Meteorology* 64 (2012).

[14] Simpson, D. et al. "The EMEP MSC-W chemical transport model – technical description." *Atmospheric Chemistry and Physics* 12 (2012): 7825-7865.

[15] Grell, G.A. et al. "Fully Coupled "Online" Chemistry within the WRF Model." *Atmospheric Environment* 39 (2005): 6957-6975. doi:10.1016/j.atmosenv.2005.04.027.

[16] ASPB. "Avaluació de la qualitat de l'aire a la ciutat de Barcelona. Informe 2018" (2018). Available on `https://www.aspb.cat/wp-content/uploads/2019/09/Informe_qualitat-aire-2018.pdf`

[17] AMB official website. `https://www.amb.cat/s/web/area-metropolitana/area-metropolitana.html`

[18] Guevara,M. et al. "Improved system for modelling Spanish emissions: HERMESv2.0." Atmos. Environ. 81, 209–221. https://doi.org/10.1016/j.atmosenv.2013.08.053.

[19] ASPB. "Avaluació de la qualitat de l'aire a la ciutat de Barcelona. Informe 2019" (2019) `https://www.aspb.cat/wp-content/uploads/2019/09/Informe_qualitat-aire-2019.pdf`

[20] WHO. "Health risks of air pollution in Europe – HRAPIE project. Recommendations for concentration–response functions for cost–benefit analysis of particulate matter, ozone and nitrogen dioxide" (2013).

[21] WHO. "Air quality guidelines global update 2005" (2005).

[22] MPRCMD, 2020a. *Ministerio de la Presidencia, Relaciones con las Cortes y Memoria Democrática*. "Real Decreto 463/2020de 14 de marzo, por el que se declara el estado de alarma para la gestión de la situación de crisis sanitaria ocasionada por el COVID-19." `https://www.boe.es/eli/es/rd/2020/03/14/463/con`.

[23] MPRCMD, 2020b. *Ministerio de la Presidencia, Relaciones con las Cortes y Memoria Democrática.* "Real Decreto-ley 10/2020, de 29 de marzo, por el que se regula un permiso retribuido recuperable para las personas trabajadoras por cuenta ajena que no presten servicios esenciales, con el fin de reducir la movilidad de la población en el contexto de la lucha contra el COVID-19." `https://www.boe.es/buscar/doc.php?id=BOE-A-2020-4166`.

[24] ASPB. "Avaluació de la qualitat de l'aire a la ciutat de Barcelona. Informe 2020" (2020) https://www.aspb.cat/wp-content/uploads/2019/09/Informe_qualitat-aire-2020.pdf

[25] Baldasano, José M. "COVID-19 lockdown effects on air quality by NO_2 in the cities of Barcelona and Madrid (Spain)." *The Science of the total environment* vol. 741 (2020): 140353. doi:10.1016/j.scitotenv.2020.140353

[26] Querol, X. et al. "PM_{10} and $PM_{2.5}$ source apportionment in the Barcelona Metropolitan area, Catalonia, Spain," *Atmospheric Environment* vol. 35, No. 36 (2001): 6407-6419. doi:10.1016/S1352-2310(01)00361-2

[27] XVPCA official website: http://mediambient.gencat.cat/ca/05_ambits_dactuacio/atmosfera/qualitat_de_laire/avaluacio/xarxa_de_vigilancia_i_previsio_de_la_contaminacio_atmosferica_xvpca/index.html

[28] Alves, C. A. et al. "Chemical profiling of PM_{10} from urban road dust." *The Science of the total environment* vol. 634 (2018): 41-51. doi:10.1016/j.scitotenv.2018.03.338

[29] Perrino C. et al. "Chemical Composition of PM_{10} in 16 Urban, Industrial and Background Sites in Italy." *Atmosphere* no. 11 (2020):479. doi:10.3390/atmos11050479

[30] Shen, Zhenxing et al. "Chemical composition of PM_{10} and $PM_{2.5}$ collected at ground level and 100 meters during a strong winter-time pollution episode in Xi'an, China." *Journal of the Air & Waste Management Association (1995)* vol. 61,11 (2011): 1150-9. doi:10.1080/10473289.2011.608619

[31] Houghton, J.T. et al. "Climate change 1995; The science of climate change". *IPPC* Cambridge University Press (1995).

[32] Sillman, S. "Tropospheric ozone and photochemical smog" *Treatise on Geochemistry* Vol. 9: Environmental Geochemistry, Ch. 11 (2003). http://www.TreatiseOnGeochemistry.com

[33] "Ozone dynamics in the Mediterranean Basin: A collection of scientific papers resulting from the MECAPIP, RECAPMA and SECAP Projects". Air Pollution Report 78, DG RTD I.2, LX 46 2/82, Brussels, 2002.

[34] Sillman, S. "The relation between ozone, NOx and hydrocarbons in urban and polluted rural environments." *Atmospheric Environment* vol 33(12) (1999): 1821-1845. http://www-personal.engin.umich.edu/~sillman

[35] EEA. "Tropospheric Ozone in EU - The consolidated report" (1998)

[36] Dumont, G. "Effects of short term measures to reduce ambient ozone concentrations in Brussels and in Belgium". Paper presented at the Ministerial Conference on Tropospheric Ozone in Northwest Europe, London, UK (1996).

[37] Hersbach, H. and Dee, D. "ERA-5 Reanalysis Is in Production". *ECMWF Newsletter* no 147 (2016).

[38] Marsh, D. et al. "Climate change from 1850 to 2005 simulated in CESM1(WACCM)". *Journal Of Climate* vol 26 (2013): 7372-7391. doi:10.1175/JCLI-D-12-00558.1

[39] Granier, C. et al. "The Copernicus Atmosphere Monitoring Service global and regional emissions." *Copernicus Atmosphere Monitoring Service (CAMS) report (2019).* doi:10.24380/d0bn-kx16

[40] Guevara, M. "HERMESv3, a stand-alone multi-scale atmospheric emission modelling framework – Part 1: global and regional module". *Geoscientific Model Development* vol. 12 (2019):1885–1907 doi:10.5194/gmd-12-1885-2019

[41] Guevara, M. et al. "Time-resolved emission reductions for atmospheric chemistry modelling in Europe during the COVID-19 lockdowns." *Atmospheric Chemistry and Physics* vol 21 (2021): 773-797. doi:10.5194/ACP-21-773-2021

[42] METEOCAT. "Butlletí Climàtic Mensual. Març del 2020" (2021). `https://static-m.meteo.cat/wordpressweb/wp-content/uploads/2021/03/01155111/Butllet%C3%AD-Marc2020_v3.pdf`

[43] METEOCAT. "Butlletí Climàtic Mensual. Abril del 2020" (2021). `https://static-m.meteo.cat/wordpressweb/wp-content/uploads/2021/03/01155111/Butllet%C3%AD-Abril2020_v3.pdf`

[44] Querol, Xavier et al. "Lessons from the COVID-19 air pollution decrease in Spain: Now what?." *The Science of the total environment* vol. 779 (2021): 146380. doi:10.1016/j.scitotenv.2021.146380

[45] Giordano, Lea et al. "Assessment of the MACC reanalysis and its influence as chemical boundary conditions for regional air quality modeling in AQMEII-2." Atmospheric Environment 115 (2015): 371-388.